Resonance fluorescence in driven quantum dots: Electron and photon correlations

Rafael Sánchez,[1,2] Gloria Platero,[1] and Tobias Brandes[3]
[1]*Instituto de Ciencia de Materiales de Madrid (CSIC), Cantoblanco, 28049 Madrid, Spain*
[2]*Dèpartement de Physique Théorique, Université de Genève, CH-1211 Gèneve 4, Switzerland*
[3]*Institut für Theoretische Physik, Technische Universität Berlin, D-10623 Berlin, Germany*
(Received 25 March 2008; revised manuscript received 15 July 2008; published 8 September 2008)

We study the counting statistics for electrons and photons being emitted from a driven two-level quantum dot. Our technique allows us to calculate their mutual correlations as well. We study different transport configurations by tuning the chemical potential of one of the leads to find that the electronic and photonic fluctuations can be externally manipulated by tuning the ac and transport parameters. We also propose special configurations where electron-photon correlation is maximal meaning that spontaneous emission of photons with a well-defined energy is regulated by single electron tunneling. Interesting features are also obtained for energy-dependent tunneling.

DOI: 10.1103/PhysRevB.78.125308 PACS number(s): 73.63.Kv, 42.50.Lc, 72.70.+m, 78.67.Hc

I. INTRODUCTION

Quantum dots (QDs) offer an ideal playground for testing coherent and quantum optical effects in an artificially designed solid-state environment,[1] with the additional benefit of having electronic transport[2,3] as a "spectroscopy" by coupling to external fermionic reservoirs and counting the flow of single electrons. Complex behavior emerges through electron-electron interactions and the interaction between electrons and other bosonic excitations such as photons[4] or phonons.[5]

The exchange of ideas between mesoscopic transport and quantum optics has turned out to be quite fruitful. For instance, thermal electron antibunching was observed experimentally by performing Hanbury Brown–Twiss-type experiments in mesoscopic conductors.[6] This fermionic antibunching has also been used for regular photon sources in *p-n* junctions[7] and quantum dots.[8,9] Reversely, bosonic statistics can be studied in quantum conductors such as beam splitters,[10] nanoelectromechanical systems,[11] or quantum point contacts,[12] where photon antibunching was predicted.[13] Another example is coherent population trapping and dark states in multilevel atoms,[14,15] originally proposed for driven three level quantum dots[16] and then extended to triple quantum dots in a simple triangle configuration.[17]

Quantum transport also benefits from the adoption of theoretical tools that are well established in quantum optics. Specially relevant in the last years has been the development of noise[18,19] and full counting statistics[20–22] for electrons. Here, many of the relevant ideas and techniques were, in fact, originally developed in quantum optics in the context of counting single photons that are emitted from a single atomic source.[23–28] Recently, electronic counting statistics has become experimentally accessible for incoherent transport through QD systems by the analysis of the time-resolved current flowing through a quantum point contact electrostatically coupled to them.[29–32] However, the back action of the quantum point contact on the QD destroys its internal coherence. Though traces of coherence have been measured in shot noise through stacks of double quantum dots,[33] the access to higher order cumulants is still a challenging problem.

Our aim in this work is to study the influence of electronic transport on the photonic emission statistics in a quantum dot system and vice versa. Two-level systems give particularly interesting features both for optical and transport quantities; in optics, resonance fluorescence in two-level atoms is the simplest case of a quantum photon source where photon antibunching occurs.[34] In transport, quantum dots with two or more capacitively coupled levels show electronic bunching in dynamical channel blockade configuration.[35] As will be shown, these properties can be studied in a two-level quantum dot which is illuminated by a resonant ac electric field, where bosonic resonance fluorescence (due to phonon or photon-mediated relaxation processes) is modified by electronic transport, and dynamical channel blockade depends on both coupling to a boson bath[36] and the driving parameters.[37]

We show how the *combined* statistics of fermions and bosons is a very sensitive tool for extracting information from time dependent driven systems. In particular, phonon emission has been measured by its influence on the electronic current in two-level systems.[38] We analyze the electron and photon noises and find that they can be tuned back and forth between sub- and super-Poissonian characters by using the strength of an ac driving field or the bias voltage. For this purpose, we develop a general method to simultaneously extract the full counting statistics of single electron tunneling and (boson mediated) relaxation events, as well as their mutual correlations.

This paper is organized as follows. In Sec. II we present our system and how to obtain the counting statistics of electrons and photons which are calculated in Secs. III–V for different chemical potentials in the right lead. In Sec. VI, we present a special configuration where electron-boson correlation is maximal. The energy-dependent tunneling case is studied in Sec. VII. Finally, Sec. VIII presents our conclusions. Due to the length of some of the analytical results, we include some appendixes with the coefficients that allow their calculation.

II. MODEL AND TECHNIQUE

Our system consists of a two-level QD connected to two fermionic leads by tunnel barriers. The Coulomb repulsion

inside the QD is assumed to be so large that only single occupation is allowed (*Coulomb blockade* regime). The lattice vibrations induce, at low temperatures, inelastic transitions from the upper to the lower state. In analogy to resonance fluorescence in quantum optics, a time-dependent ac field with a frequency ω drives the transition between the two levels ε_1 and ε_2 close to resonance, $\Delta_\omega=\varepsilon_2-\varepsilon_1-\omega\approx 0$ (we will consider $e=\hbar=1$ through the whole text), which allows us to assume the rotating wave approximation. Thus, the electron in the QD is coherently delocalized between both levels performing *photon-assisted Rabi oscillations*.[4,39] For simplicity, we consider spinless electrons. Studies of spin currents in a quantum dot coupled to a quantized driving or an ac magnetic field can be found in Refs. 40 and 41, respectively.

This system is modeled by the Hamiltonian,

$$\hat{H}(t)=\sum_i \varepsilon_i \hat{d}_i^\dagger \hat{d}_i+\frac{\Omega}{2}(e^{-i\omega t}\hat{d}_2^\dagger \hat{d}_1+\text{H.c.})+\sum_{k\sigma}\varepsilon_{k\alpha}\hat{c}_{k\alpha}^\dagger \hat{c}_{k\alpha}+\sum_{k\alpha i}V_{\alpha i}(c_{k\alpha}^\dagger \hat{d}_i+\text{H.c.})+\sum_{q,\nu}\omega_q \hat{a}_{q\nu}^\dagger \hat{a}_{q\nu}+\sum_{ij,q\nu}\lambda_{q\nu}^{ij}\hat{d}_i^\dagger \hat{d}_j(\hat{a}_{-q\nu}+\hat{a}_{q\nu}^\dagger), \tag{1}$$

where $\hat{a}_{q\nu}$, $\hat{c}_{k\alpha}$, and $\hat{d}_i$ are annihilation operators of bosons (with momentum q and polarization ν) and electrons in the lead α and in the level i of the QD, respectively, and Ω is the Rabi frequency, which is proportional to the intensity of the ac field.

The terms proportional to $V_{\alpha i}$ and $\lambda_{q\nu}^{ij}$ in Eq. (1) give the coupling of the electrons in the QD to the fermionic leads and their interaction with the bosonic bath, respectively. In the following, we assume a basis of quantum dot levels where diagonal matrix elements of $\lambda_{q\nu}^{ij}$ play a minor role and we set $\lambda_{q\nu}^{ii}=0$. For coupling to photons, this would correspond to a usual dipole interaction with the electromagnetic field. For phonons, this is justified if we are mainly interested in weak-coupling and relaxation processes by spontaneously emitted bosons in the relaxation from the upper to the lower level. The electron-boson coupling term, in the rotating wave approximation, can then be written as $\Sigma_{q\nu}\lambda_{q\nu}(\hat{d}_2^\dagger \hat{d}_1 \hat{a}_{q\nu}+\text{H.c.})$. For the sake of illustrating our results with concrete physical processes we will refer to *photon emission* in the following, i.e., the bosonic bath corresponds to the photon vacuum without additional coupling to phonons. Finally, the coupling to the fermionic and bosonic bath terms is responsible for the incoherent dynamics and they can be considered apart in the derivation of the master equation for the reduced density matrix.

Considering the quantum-jump approach[42,43] to electronic transport and boson emission events, the equation of motion of the reduced quantum dot density matrix can be written as

$$\dot{\rho}(t)=\mathcal{L}_0(t)\rho(t)+\mathcal{L}_e(t)\rho(t)+\mathcal{L}_p(t)\rho(t), \tag{2}$$

where $\mathcal{L}_e$ and $\mathcal{L}_p$ are the Liouvillian *jump* superoperators responsible for the incoherent events: electron tunneling from the system to the collector and relaxation by spontaneous photon emission. Thus, we can consider a density matrix resolved in the number of accumulated electrons in the collector, n_e, and the number of emitted photons, n_p,

$$\rho(t)=\sum_{n_e,n_p}\rho^{(n_e,n_p)}(t), \tag{3}$$

where $\rho^{(n_e,n_p)}(t)$ gives the probability that, during a certain time interval t, n_e electrons have tunneled out of a given electron-photon system and n_p photons have been emitted.

This allows us to define the generating function,[28]

$$G(t,s_e,s_p)=\sum_{n_e,n_p}s_e^{n_e}s_p^{n_p}\rho^{(n_e,n_p)}(t), \tag{4}$$

by introducing the electron (photon) counting variables, $s_{e(p)}$. The derivatives of $G(t,s_e,s_p)$ with respect to the counting variables give the correlations

$$\frac{\partial^{\ell+m}\,\text{tr}\,G(t,1,1)}{\partial s_e^\ell\,\partial s_p^m}=\left\langle\prod_{i=1}^{\ell}\prod_{j=1}^{m}(n_e-i+1)(n_p-j+1)\right\rangle \tag{5}$$

up to any order.

One can derive the equations of motion for the generating function as previously done for the density matrix,

$$\dot{G}(t,s_e,s_p)=M(s_e,s_p)G(t,s_e,s_p), \tag{6}$$

which generalizes the master equation, $\dot{\rho}(t)=M(1,1)\rho(t)$. The jump superoperators affect only the diagonal elements of the generating function in the same way that rate equations involve only the occupation probabilities—given by the diagonal elements of the density matrix. The electronic one acts as

$$[\mathcal{L}_e(t)G(t,s_e,s_p)]_{mm}=\sum_k(s_e\Gamma_{mk}^+ +s_e^{-1}\Gamma_{mk}^-)G_{kk}(t,s_e,s_p), \tag{7}$$

where $\Gamma_{mk}^\pm$ is the rate for processes that increase/decrease the number of electrons in the collector by a transition from state $|k\rangle$ to state $|m\rangle$. The same can be done for photons, with the difference that the number of detected photons can only increase. Then, one only has to introduce the corresponding counting variables in those terms corresponding to the tunneling of an electron to the collector lead and the emission of a photon. The relevant elements of the density matrix can be written as a vector, $\rho=(\rho_{00},\rho_{11},\rho_{12},\rho_{21},\rho_{22})^T$, where ρ_{00} gives the occupation of the empty state, ρ_{11} and ρ_{22} correspond to the ground and excited electronic states, respectively, and ρ_{12} and $\rho_{21}=\rho_{12}^*$ are the coherences. Then, for the case where the tunneling barriers are equal for both energy levels, i.e., $V_{\alpha 1}=V_{\alpha 2}$, the equation of motion of the generating function (6) is described, in the Born-Markov approximation, by the matrix[44,45]

$$M(s_e,s_p)=\begin{pmatrix} -2\Gamma_L-(f_1+f_2)\Gamma_R & s_e\bar{f}_1\Gamma_R & 0 & 0 & s_e\bar{f}_2\Gamma_R \\ \Gamma_L+s_e^{-1}f_1\Gamma_R & -\bar{f}_1\Gamma_R & i\frac{\Omega}{2} & -i\frac{\Omega}{2} & s_p\gamma \\ 0 & i\frac{\Omega}{2} & \Lambda_{12}+i\Delta_\omega & 0 & -i\frac{\Omega}{2} \\ 0 & -i\frac{\Omega}{2} & 0 & \Lambda_{12}-i\Delta_\omega & i\frac{\Omega}{2} \\ \Gamma_L+s_e^{-1}f_2\Gamma_R & 0 & -i\frac{\Omega}{2} & i\frac{\Omega}{2} & -\gamma-\bar{f}_2\Gamma_R \end{pmatrix}, \tag{8}$$

where, by further considering that the density of states in the leads is rather constant so $d_\alpha(\omega_{mn})=d_\alpha$, the tunneling rates through the left (right) lead are equal to $\Gamma_{L(R)}=2\pi d_{L(R)}|V_{L(R)}|^2$. We will consider a high bias configuration where the chemical potential of the left lead is well above the energy levels and the transitions between the right lead (with a chemical potential μ) and the state i in the QD are weighted by the Fermi distribution functions $f_i=f(\varepsilon_i-\mu)=(1+e^{(\varepsilon_i-\mu)\beta})^{-1}$ and $\bar{f}_i=1-f_i$. γ is the spontaneous emission rate due to the coupling with the photon bath: $\gamma=2\pi\Sigma_\nu\int d^3q g(q)|\lambda_{q\nu}|^2\delta(|q|v-\varepsilon_2+\varepsilon_1)$, where $g(q)$ is the density of states.[45] The decoherence is given by $\Lambda_{12}=-\frac{1}{2}[(\bar{f}_1+\bar{f}_2)\Gamma_R+\gamma]$. The Fermi energy of the left lead is considered high enough that no electrons can tunnel from the QD to the left lead. All the parameters in these equations, except the sample-depending coupling to the photon bath, can be externally manipulated.

Taking the Laplace transform of the generating function, $\tilde{G}(z,s_e,s_p)=(z-M)^{-1}\rho(0)$, where $\rho(0)$ is the initial state, the long-time behavior is given by the residue for the pole near $z=0$. From the Taylor expansion of the pole $z_0=\Sigma_{m,n>0}c_{mn}(s_e-1)^m(s_p-1)^n$, one can write $\mathrm{tr}\,G(t,s_e,s_p)\sim g(s_e,s_p)e^{z_0t}$ and obtain, from Eq. (5), the mean value, $\langle n_{e(p)}\rangle$, as well as the higher order cumulants, $\kappa^{(i)}_{e(p)}=\langle(n_{e(p)}-\langle n_{e(p)}\rangle)^i\rangle$,

$$\kappa^{(2)}_{e(p)}=\frac{\partial^2 g(1,1)}{\partial s^2_{e(p)}}-\left(\frac{\partial g(1,1)}{\partial s_{e(p)}}\right)^2+(c_{10(01)}+2c_{20(02)})t, \tag{9a}$$

$$\kappa^{(3)}_{e(p)}=\frac{\partial^3 g(1,1)}{\partial s^3_{e(p)}}-3\frac{\partial g(1,1)}{\partial s_{e(p)}}\frac{\partial^2 g(1,1)}{\partial s^2_{e(p)}}+2\left(\frac{\partial g(1,1)}{\partial s_{e(p)}}\right)^3+\frac{\partial g(1,1)}{\partial s_{e(p)}}+(c_{10(01)}+6c_{20(02)}+6c_{30(03)})t, \tag{9b}$$

which give the variance and skewness of the probability distribution, respectively. In the large time asymptotic limit, all the information is included in the coefficients c_{mn}. Thus, we obtain the stationary current and the low-frequency noise,

$$I_{e(p)}=\frac{d}{dt}\langle n_{e(p)}\rangle=c_{10(01)}, \tag{10}$$

$$S_{e(p)}(0)=\frac{d}{dt}\kappa^{(2)}_{e(p)}=c_{10(01)}+2c_{20(02)}, \tag{11}$$

respectively. Then, the Fano factor is $F_{e(p)}=1+2c_{20(02)}/c_{10(01)}$ so that the sign of the second term in the right-hand side defines the sub-($F<1$) or super-($F>1$) Poissonian character of the noise.

In the limit $\Gamma_{L(R)}\to 0$, the pure resonance fluorescence case for the noise of the emitted photons, formally equivalent to the expression for emitted photons in quantum optics,[28] is obtained,

$$F_p(\Gamma_i=0)=1-\frac{2\Omega^2(3\gamma^2-4\Delta_\omega^2)}{(\gamma^2+2\Omega^2+4\Delta_\omega^2)^2}, \tag{12}$$

yielding the famous sub-Poissonian noise result at resonance ($\Delta_\omega=0$). The detuning between the frequency of the ac field and the level energy separation, Δ_ω, contributes to *restore* super-Poissonian statistics, as seen in Fig. 2. In the following, only the resonant case will be considered unless the opposite was indicated.

Electron-photon correlations are obtained from

$$\langle n_e n_p\rangle=\frac{\partial g(1,1)}{\partial s_e}c_{01}t+\frac{\partial g(1,1)}{\partial s_p}c_{10}t+c_{11}t+c_{10}c_{01}t^2. \tag{13}$$

Then, by defining $\sigma^2_{ij}=\langle n_i n_j\rangle-\langle n_i\rangle\langle n_j\rangle$, where $\sigma^2_{ii}=\kappa^{(2)}_i$,

$$\sigma^2_{ep}=\frac{\partial^2 g(1,1)}{\partial s_e\,\partial s_p}+c_{11}t \tag{14}$$

defines the variance between electronic and photonic events. The long-time behavior is given by $\sigma^2_{ep}\sim c_{11}t$ so the correlation coefficient can then be defined as[46]

$$r=\frac{\sigma_{ep}}{\sqrt{\sigma^2_{ee}\sigma^2_{pp}}}=\frac{c_{11}}{\sqrt{(c_{10}+2c_{20})(c_{01}+2c_{02})}}. \tag{15}$$

Similarly to the electronic (photonic) correlations, where the sign of the second-order cumulant, $c_{20(02)}$, defined the sub- or super-Poissonian character of the noise, the sign of

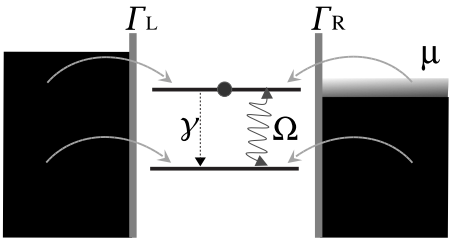

FIG. 1. When the chemical potential in the right lead μ is above the energy of both levels, the electron remains in the quantum dot and photons are spontaneously emitted analogously as photons in resonance fluorescent atoms.

c_{11} gives the character of the electron-photon correlations. If $c_{11}>0$, the detection of a transmitted electron would involve the detection of a photon in a short lapse of time, while $c_{11}<0$ involves distant events.

The electron-photon correlation coefficient is limited to $|r|<1$, having $r=1$ for the case where the number of detected electrons is proportional to the number of detected photons: $n_e \propto n_p$. $r=0$ means uncorrelated events. Note that independent events give $r=0$, but the opposite is not necessarily true, as will be shown below. Analogously to the Fano factor for the second-order cumulants, the deviation of the third cumulants from the Poissonian statistics can be parametrized by the coefficient

$$\eta_{e(p)} = \frac{1}{I_{e(p)}}\frac{d}{dt}\kappa^{(3)}_{e(p)} = 1 + 6\frac{c_{20(02)} + c_{30(03)}}{c_{10(01)}}. \tag{16}$$

In what follows, different configurations will be discussed concerning the relative positions of the energy levels with respect to the chemical potentials of the contacts. As will be shown, electron and photon fluctuations and their correlations are strongly sensitive to the concrete configuration of the system.

III. RESONANCE FLUORESCENCE LIMIT

The chemical potential of the left lead is considered to be well above the energies of the QD, so it can be considered infinite. If the chemical potential of the right lead, μ, is also above the energies of both levels, $\mu>\varepsilon_{1(2)}$, the QD is always populated by one electron and transport is canceled. Then, this case is completely analogous to the resonance fluorescence problem, where spontaneously emitted photons play the role of fluorescent photons; the trapped electron is coherently delocalized by the driving field between the two levels performing photoassisted Rabi oscillations until the emission of a photon, then the electron is relaxed to the lower level (cf. Fig. 1).

We consider a small correction to this behavior due to the thermal smearing of the Fermi level for finite temperatures. Then, there is a contribution of transport by a small but finite probability for the electron to be extracted to the right lead when it occupies the upper level. The Fermi distribution function weighing this transition can be approximated by $\bar{f}_2 = x \approx e^{\beta(\varepsilon_2-\mu)}$, where $\beta=(k_BT)^{-1}$ (see Fig. 1). The effect of thermal smearing on electronic transport through a quantum dot has been controlled recently.[47] Then, photons deviate from the resonance fluorescence like statistics because the QD may be empty during short lapses of time. It would be the case if the resonance fluorescent atom could be eventually ionized. Then, from the Taylor expansion for low x, one obtains a finite electronic current,

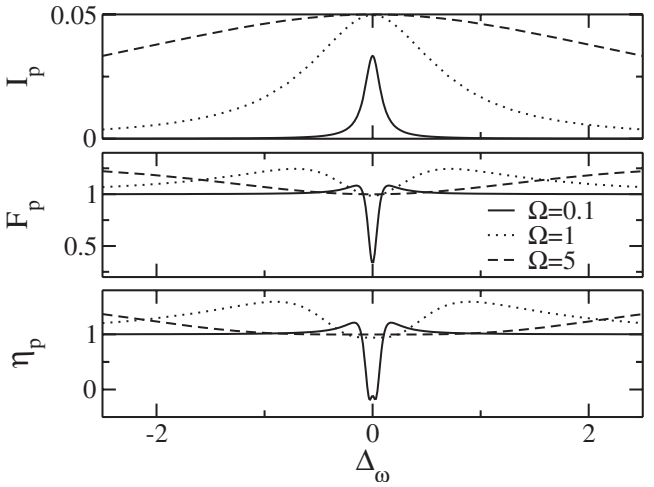

FIG. 2. $\mu \gtrsim \varepsilon_2$: dependence of the photonic current, Fano factor, and skewness with the detuning for different field intensities in the regime where no levels are in the transport window: $\varepsilon_{1,2}<\mu$. $\Gamma_L=\Gamma_R=\Gamma=1$, $\gamma=0.1$, and $x\approx 0$. Since electronic transport is canceled in this regime, the photonic statistics are equivalent to the resonance fluorescence problem. Sub-Poissonian photonic statistics are only found near resonance. It must be noted here, however, that the validity of these results, obtained within the rotating wave approximation, is guaranteed only for $\Delta_\omega \approx 0$.

$$I_e = \frac{\Omega^2\Gamma_L\Gamma_R}{(\gamma^2+2\Omega^2)(\Gamma_L+\Gamma_R)}x + O(x^2), \tag{17}$$

which introduces a small contribution in the photonic emission,

$$I_p = \frac{\gamma\Omega^2}{\gamma^2+2\Omega^2} - \frac{\gamma\Omega^2\Gamma_R[\Omega^2+3\gamma(\Gamma_L+\Gamma_R)]}{2[(\gamma^2+2\Omega^2)^2(\Gamma_L+\Gamma_R)]}x + O(x^2). \tag{18}$$

The photonic resonance fluorescence behavior, as well as electronic transport quenching, is recovered for $x=0$ (cf. Fig. 2). There, it can be seen that the sub-Poissonian photon behavior goes super-Poissonian in the vicinity of the resonance, as described by Eq. (12). In those regions and opposite to what is seen in resonance, the ac intensity increases the deviation of the statistics from the Poissonian values. From Eqs. (17) and (18) and the expressions shown in Appendix A for the second-order moments, one obtains the contribution of the thermal smearing of the collector in the electronic statistics (for $\Gamma_L=\Gamma_R=\Gamma$) and the expected photonic Fano factor,

$$F_e = 1 + \frac{1}{4}\left(\frac{2\gamma\Gamma(\gamma^2-2\Omega^2)}{(\gamma^2+2\Omega^2)^2} - \Omega^2\right)x + O(x^2), \tag{19}$$

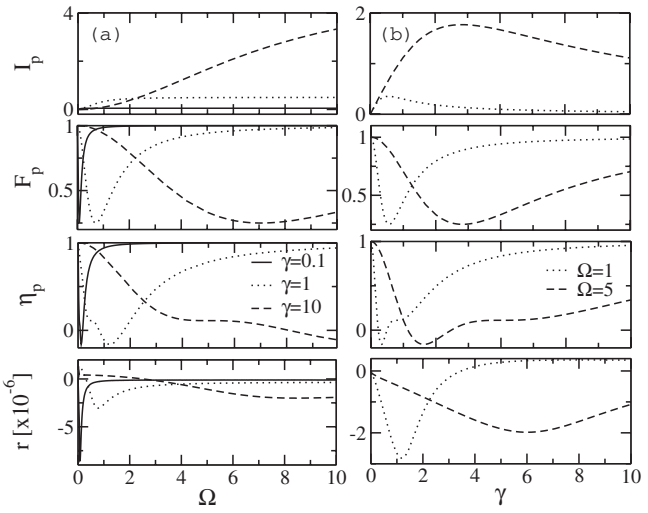

FIG. 3. $\mu \gtrsim \varepsilon_2$: dependence of the photonic current, Fano factor, and skewness and the electron-photon correlation with (a) the field intensity, Ω, for different photon emission rates and (b) the photon emission rate, γ, for different field intensities in the regime where no levels are in the transport window: $\varepsilon_{1,2} < \mu$. $\Gamma_L = \Gamma_R = \Gamma = 1$ and $x \approx 0$. F_p and η_p show a pronounced minimum in their dependence with the field intensity typical for resonance fluorescence. In the nondriven case, $I_p = 0$, $F_p = \eta_p = 1$, and $r = 0$.

$$F_p = 1 - \frac{6\gamma^2\Omega^2}{(\gamma^2 + 2\Omega^2)^2} + O(x). \tag{20}$$

The driving field induces sub-Poissonian photonic noise which (in the limit $x=0$) reaches a minimum $F_{p,m} = \frac{1}{4}$ for $\Omega_m = \gamma/\sqrt{2}$ before the Rabi oscillations dominate the dynamics over relaxation processes (cf. Fig. 3). The electron-photon correlation coefficient becomes (see Appendix A)

$$r = [2\Gamma\gamma(\gamma^2 - 10\Omega^2) - \Omega^2(\gamma^2 + 2\Omega^2)] \times \sqrt{\frac{\gamma x}{16\Gamma(\gamma^4 - 2\Omega^2\gamma^2 + 4\Omega^4)}} + O(x^{3/2}), \tag{21}$$

where it is clear that the ac field contributes to negative electron-photon correlations (cf. Fig. 3). The third cumulants become

$$\eta_e = 1 + \frac{3}{4}\left(\frac{2\gamma\Gamma(\gamma^2 - 4\Omega^2)}{(\gamma^2 + 2\Omega^2)^2} - \frac{\Omega^2}{\gamma^2 + 2\Omega^2}\right)x + O(x^2) \tag{22}$$

for electrons and

$$\eta_p = 1 - \frac{6\Omega^2\gamma^2(3\gamma^4 - 4\Omega^2\gamma^2 + 16\Omega^4)}{(\gamma^2 + 2\Omega^2)^4} + O(x) \tag{23}$$

for photons.

Interestingly, the strong photonic noise suppression coincides with a region where the skewness almost vanishes [cf. Fig. 3(a)], leading to the possibility to operate the device as a *regular boson source*. Two asymptotic limits of the results presented above, the undriven and high-field intensity limits, will be considered.

A. Undriven case: $\Omega = 0$

In the absence of driving, once an electron occupies the lower level—by direct tunneling from the leads or by relaxation from the upper one—there is no process able to remove the electron from the lower level. Then, the stationary state of the system coincides with $\rho_2 = 1$ and both photon emission and electron tunneling are canceled,

$$c_{ij} = 0 \quad \forall\, i,j. \tag{24}$$

As expected, the cancellation of photon emission makes all the photonic cumulants Poissonian, so $F_p = \eta_p = 1$. However, a small contribution of the tunneling through the upper level modifies the electronic shot noise, so the Fano factor

$$F_e = 1 + \frac{2x\Gamma_L\Gamma_R}{(\Gamma_L + \Gamma_R)(2\gamma + x\Gamma_R) - x\gamma\Gamma_R} \tag{25}$$

and the skewness of the statistics

$$\eta_e = 1 + \frac{6x\Gamma_L\Gamma_R\{2\Gamma_L(\gamma + x\Gamma_R) + \Gamma_R[x\Gamma_R - (x-2)\gamma]\}}{\{\Gamma_L(2\gamma + x\Gamma_R) + \Gamma_R[x\Gamma_R - (x-2)\gamma]\}^2} \tag{26}$$

are spuriously super-Poissonian. Then, also the electron-photon correlation is affected. For the case $\Gamma_L = \Gamma_R = \Gamma$,

$$r = \sqrt{\frac{(4-x)\gamma x}{2[2x\Gamma + (4-x)\gamma][4x\Gamma + (4-x)\gamma]}}. \tag{27}$$

All these deviations are obviously canceled as the rate for extracting an electron from the upper level, $x\Gamma_R$, goes to zero.

B. High intensity limit: $\Omega \to \infty$

Increasing the intensity of the ac field, the electron tends to occupy the upper level with a probability: $\rho_2 = \frac{2\Gamma_L + (2-x)\Gamma_R}{4\Gamma_L + (4-x)\Gamma_R}$ ($\sim \frac{1}{2}$ when $x \to 0$). Then, it can tunnel to the right contact (with a probability $x\Gamma_R$) or be relaxed to the lower level (with a probability γ), contributing to finite electronic and photonic currents,

$$I_e = \frac{2x\Gamma_L\Gamma_R}{4\Gamma_L + (4-x)\Gamma_R}, \tag{28}$$

$$I_p = \frac{\gamma[2\Gamma_L + (2-x)\Gamma_R]}{4\Gamma_L + (4-x)\Gamma_R}. \tag{29}$$

The electronic dynamics is then quite similar to the single resonant-level case,[48] so the Fano factor becomes slightly sub-Poissonian,

$$F_e = 1 - \frac{8x\Gamma_L\Gamma_R}{[4\Gamma_L + (4-x)\Gamma_R]^2}. \tag{30}$$

Since the occupation probability of the upper level at high-field intensity is maximum, so it is the probability of finding the QD unoccupied, $\rho_0 = \frac{x\Gamma_R}{4\Gamma_L + (4-x)\Gamma_R}$, after the extraction of the electron to the right lead. This introduces lapses of time when photon emission is suppressed, affecting the pho-

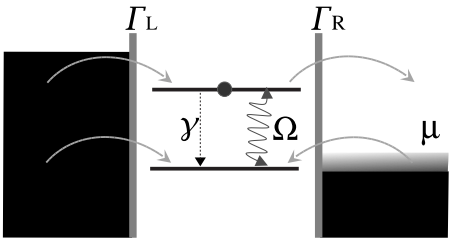

FIG. 4. Dynamical channel blockade configuration, where the electronic transport is strongly suppressed through the lower level, though there is a small probability introduced by thermal smearing of the Fermi surface in the right lead. Again, the chemical potential of the left lead is considered infinite.

tonic statistics by turning it super-Poissonian,

$$F_p = 1 + \frac{2x\gamma\Gamma_R}{[4\Gamma_L + (4-x)\Gamma_R]^2}. \tag{31}$$

On contrary, electron-photon correlation is negative since the detection of an electron (photon) reduces the probability of detecting a photon (electron): when an electron has tunneled out of the system (therefore the quantum dot is empty), photon emission is suppressed. On the other hand, when a photon has been emitted, the upper level is unoccupied and no electron can be extracted from the quantum dot. For $\Gamma_L = \Gamma_R = \Gamma$,

$$r = -\frac{\sqrt{2x\gamma}(8-3x)}{\sqrt{(4-x)(64-24x+x^2)[2x\gamma+(8-x)^2\Gamma]}}. \tag{32}$$

For the higher moments, one obtains

$$\eta_e = 1 - \frac{24x[64-(24-x)x]}{(8-x)^4}, \tag{33}$$

$$\eta_p = 1 + \frac{6x\gamma[(8-x)^2\Gamma - (8-3x)\gamma]}{(8-x)^4\Gamma^2}. \tag{34}$$

IV. DYNAMICAL CHANNEL BLOCKADE REGIME

If the chemical potential of the right lead lies between the energy levels of the QD, $\varepsilon_1 < \mu < \varepsilon_2$ and therefore $f_1 = 1-x$, $f_2 = 0$, where $x \approx e^{\beta(\varepsilon_1-\mu)}$ and $\beta = (k_B T)^{-1}$, electronic transport is strongly suppressed through the lower level (cf. Fig. 4). Then, since only one electron is allowed in the system, the occupation of the lower level avoids the entrance of electrons from the left lead and the current is blocked. This mechanism, which is known as *dynamical channel blockade*, predicts electronic super-Poissonian shot noise in multichannel systems such as, for instance, two-level quantum dots[35] or capacitively coupled double quantum dots[36,49] as well as positive cross correlations in three terminal devices.[50] It has been proposed as the responsible of noise enhancement measured experimentally in multilevel quantum dots[51] and stacks of double quantum dots.[33]

The blocking of the current is not forever since the electron in the lower level has a finite but small probability of tunneling to the collector, $x\Gamma_R$, due to the thermal smearing of the Fermi level. Then, the trapped electron eventually escapes to the right lead allowing electrons to tunnel through the upper level before the lower one is again occupied. Thus, the current is restricted to short lapses of time while for long periods $t \sim (x\Gamma_R)^{-1}$ transport is quenched. This *bunching* of electrons is reflected in super-Poissonian shot noise.

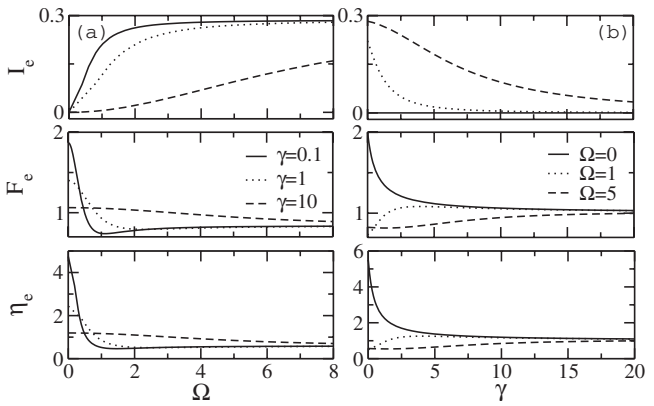

FIG. 5. Dynamical channel blockade: dependence of I_e, F_e, and η_e with (a) the field intensity, Ω, for different photon emission rates and (b) the photon emission rate, γ, for different field intensities in the dynamical channel blockade regime: $\varepsilon_1 < \mu < \varepsilon_2$. $\mu < \varepsilon_{1,2}$. $\Gamma_L = \Gamma_R = \Gamma = 1$, $\tilde{\Omega} = \Omega/\Gamma$, $\tilde{\gamma} = \gamma/\Gamma$, and $x \approx 0$. As discussed in the text, the super-Poissonian electronic Fano factor, typical for dynamical channel blockade, is turned sub-Poissonian by the ac intensity.

Photon-mediated relaxation introduces an additional way to occupy the lower level when current is flowing through the upper one, shortening the lapse of time when transport is allowed. Thus, the electrons are transferred in smaller bunches and the super-Poissonian character of the electronic noise is reduced. The detection of a photon is always at the end of a bunch of electrons and implies the cancellation of the current, leading to a positive electron-photon correlation.

The introduction of the ac field pumps the electron in the lower state to the upper one, giving the electron a finite probability to tunnel to the right lead or to be relaxed by the emission of one photon. This reduces the electronic shot noise by reducing the duration of the lapses of time when transport is blocked (opposite to the effect of photons). Thus, when $x=0$, the electronic current and the photonic emission are proportional to the driving intensity,

$$I_e = \frac{2\Omega^2\Gamma_L\Gamma_R}{\Gamma_R(\tilde{\Gamma}_R^2 + 3\Omega^2) + \Gamma_L[\tilde{\Gamma}_R(2\gamma+\Gamma_R) + 4\Omega^2]}, \tag{35}$$

$$I_p = \frac{\gamma\Omega^2(2\Gamma_L+\Gamma_R)}{\Gamma_R(\tilde{\Gamma}_R^2 + 3\Omega^2) + \Gamma_L[\tilde{\Gamma}_R(2\gamma+\Gamma_R) + 4\Omega^2]}, \tag{36}$$

and channel blockade is removed (see Figs. 5 and 6). We have defined $\tilde{\Gamma}_R = \gamma + \Gamma_R$. Considering, for simplicity, the case $\Gamma_L = \Gamma_R = \Gamma$ and $\tilde{\Gamma} = \gamma + \Gamma$, the Fano factors become (see Appendix B)

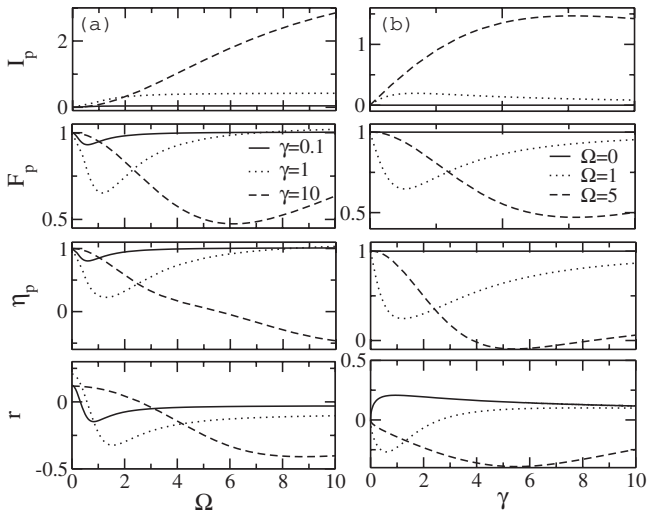

FIG. 6. Dynamical channel blockade: dependence of the photonic current, Fano factor, and skewness and the electron-photon correlation coefficient with (a) the field intensity for different photon emission rates and (b) the photon emission rate, γ, for different field intensities in the dynamical channel blockade regime: $\varepsilon_1 < \mu < \varepsilon_2$. $\mu < \varepsilon_{1,2}$. $\Gamma_L = \Gamma_R = \Gamma = 1$ and $x \approx 0$.

$$F_e = 1 - \frac{8\Omega^4 + 2(2\gamma^2 + 15\Gamma\gamma + 9\Gamma^2)\Omega^2 - 2\Gamma\tilde{\Gamma}^2(3\gamma + 2\Gamma)}{[7\Omega^2 + \tilde{\Gamma}(3\gamma + 2\Gamma)]^2} \tag{37}$$

for electrons and

$$F_p = 1 - \frac{2\gamma\Omega^2(22\Gamma^2 + 28\gamma\Gamma - \Omega^2)}{\Gamma[7\Omega^2 + \tilde{\Gamma}(3\gamma + 2\Gamma)]^2} \tag{38}$$

for photons. As can be seen in Fig. 6(a), the minimum that appeared in the resonance fluorescence configuration still appears, but its depth and position now depend on the tunneling rates. The modification of the resonance fluorescence behavior is also reflected in the super-Poissonian large ac intensity asymptotic value (discussed below).

The electron-photon correlation coefficient will be considered in the asymptotic nondriven and high-field intensity cases. As expected, the driving contributes to make the electronic noise sub-Poissonian and the photonic one super-Poissonian. However, it has to compete with the photon emission that contributes to bring the electron to the lower state and to block the current. In Fig. 5(b), it can be seen how the pumped electronic current is decreased by the photon emission rate and the Fano factor tends asymptotically to be Poissonian. The positive electron-photon correlation is decreased by the ac field since the emission of a photon does not imply transport blocking anymore, as seen in Fig. 6.

A. Undriven case: $\Omega = 0$

The most interesting features appear in the absence of the ac field, where the consequences of the dynamical channel blockade are maximal and there is a strong dependence of the statistics on the thermal smearing factor, x. In the absence of photons ($\gamma = 0$), the electronic current and Fano factor are

$$I_e = \frac{2x\Gamma_L\Gamma_R}{(x+1)\Gamma_L + \Gamma_R}, \tag{39}$$

$$F_e = 1 + \frac{2\Gamma_L[(1-x)^2\Gamma_L + (1-3x)\Gamma_R]}{[(x+1)\Gamma_L + \Gamma_R]^2}. \tag{40}$$

It is interesting to see here how the Fano factor can be tuned by the asymmetric coupling to the leads: $F_e = 3$ (if $\Gamma_L \gg \Gamma_R$), $F_e = 2$ (if $\Gamma_L = \Gamma_R$), and $F_e = 1$ (if $\Gamma_L \ll \Gamma_R$). In the latest case, the contribution of $x\Gamma_R$ is diminished and the left barrier controls the transport (in this limit, the current is $I_e = 2x\Gamma_L$). Then, the transferred electrons are uncorrelated one from the others resembling the behavior of the single barrier problem briefly discussed above. The case $\Gamma_L \gg \Gamma_R$ was studied in Ref. 35 without considering the processes that introduce an electron from the collector to the lower level, with a rate $(1-x)\Gamma_R$. These transitions do not contribute in this particular limit, but that is not the case for the rest of configurations.

Considering photon emission and small x, one can expand the first coefficients for the electronic and photonic statistics, as well as for the electron-photon correlations. Relaxation by photons contributes to shorten the bunches of electrons flowing through the upper level when the lower one is empty, thus reducing both the electronic current,

$$I_e = \frac{2\Gamma_L\Gamma_R(\gamma + \Gamma_R)x}{\Gamma_R(\gamma + \Gamma_R) + \Gamma_L(2\gamma + \Gamma_R)} + O(x^2), \tag{41}$$

and Fano factor (*noise reduction by noise*),

$$F_e = 1 + \frac{2\Gamma_L\Gamma_R}{\Gamma_R\tilde{\Gamma}_R + \Gamma_L(\gamma + \tilde{\Gamma}_R)} - 2\Gamma_L\Gamma_R\frac{\tilde{\Gamma}_R^2 + (\tilde{\Gamma}_R + 2\Gamma_L)(\gamma + 2\Gamma_R)}{[\Gamma_R\tilde{\Gamma}_R + \Gamma_L(\gamma + \tilde{\Gamma}_R)]^2}x + O(x^2), \tag{42}$$

without affecting to its super-Poissonian character [cf. Fig. 5(b)]. Again, we defined, for simplicity, $\tilde{\Gamma}_R = \gamma + \Gamma_R$. The photonic current and Fano factor become

$$I_p = \frac{\gamma\Gamma_L\Gamma_R x}{\Gamma_R(\gamma + \Gamma_R) + \Gamma_L(2\gamma + \Gamma_R)} + O(x^2), \tag{43}$$

$$F_p = 1 - \frac{2\gamma\Gamma_L\Gamma_R(\gamma + 2\Gamma_L + 2\Gamma_R)x}{[\Gamma_R(\gamma + \Gamma_R) + \Gamma_L(2\gamma + \Gamma_R)]^2} + O(x^2), \tag{44}$$

while we obtain, for the electron-photon correlation coefficient (in the case $\Gamma_L = \Gamma_R = \Gamma$),

$$r = 3\sqrt{\frac{\gamma(\gamma + \Gamma)}{(3\gamma + 2\Gamma)(3\gamma + 4\Gamma)}} + O(x). \tag{45}$$

Interestingly, the electron-photon correlation is roughly independent of x, which allows to extract information that is not provided by the *flat* photonic Fano factor [cf. Fig. 6(b)].

The expected positive electron-photon correlations are obtained. On the other hand, the presence of electronic transport affects the Poissonian photonic statistics by introducing

a sub-Poissonian component; once a photon has been emitted, the electron is relaxed to the lower level blocking the transport. A second photon will not be detected until the electron tunnels to the collector and another one enters the upper level, so photonic events are well separated in time.

From the third cumulants, one obtains

$$\eta_e = 1 + \frac{6\Gamma_L\Gamma_R(\gamma+\Gamma_R)(2\Gamma_L+\Gamma_R)}{[\Gamma_R(\gamma+\Gamma_R)+\Gamma_L(2\gamma+\Gamma_R)]^2} + O(x), \quad (46)$$

$$\eta_p = 1 - \frac{6[\gamma\Gamma_L\Gamma_R(\gamma+2\Gamma_L+2\Gamma_R)]x}{[\Gamma_R(\gamma+\Gamma_R)+\Gamma_L(2\gamma+\Gamma_R)]^2} + O(x^2). \quad (47)$$

B. High intensity limit: $\Omega \to \infty$

If the intensity of the driving field is large enough, the dynamical channel blockade is completely lifted, finding electronic and photonic currents,

$$\frac{I_e}{2(1+x)\Gamma_L\Gamma_R} = \frac{I_p}{\gamma[2\Gamma_L+(1-x)\Gamma_R]} = \frac{1}{4\Gamma_L+(3-x)\Gamma_R}, \quad (48)$$

so sub-Poissonian electronic noise and super-Poissonian photonic noise are recovered,

$$F_e = 1 - \frac{8\Gamma_L\Gamma_R}{(4\Gamma_L+3\Gamma_R)^2} + O(x), \quad (49)$$

$$F_p = 1 + \frac{2\gamma\Gamma_R}{(4\Gamma_L+3\Gamma_R)^2} + O(x). \quad (50)$$

Interestingly, in this regime, the photonic influence is washed out from the electronic statistics. Also, the ac field allows the extraction through the upper level of an electron that has been relaxed by the emission of one photon. This means that the electron-photon correlation becomes negative (for $\Gamma_L = \Gamma_R = \Gamma$),

$$r = -5\sqrt{\frac{2\gamma}{123(2\gamma+49\Gamma)}} + O(x). \quad (51)$$

Then, by tuning the driving intensity, one can manipulate the character of the shot noise of electrons and photons, turning the super- (sub-)Poissonian statistics to sub- (super-)Poissonian for electrons (photons) when increasing Ω. Higher moments are also obtained, giving

$$\eta_e = 1 - \frac{24(x+1)[41-(22-x)x]}{(7-x)^4}, \quad (52)$$

$$\eta_p = 1 + \frac{6(x+1)\gamma[(7-x)^2\Gamma-(5-3x)\gamma]}{(7-x)^4\Gamma^2}. \quad (53)$$

V. BOTH LEVELS IN THE TRANSPORT WINDOW REGIME

If the energy of both levels are above μ, $\varepsilon_1, \varepsilon_2 > \mu$ ($f_1 = f_2 = 0$), the two of them contribute to electronic transport

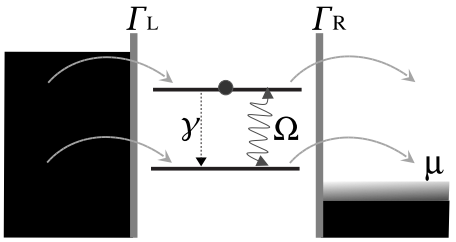

FIG. 7. System configuration discussed in Sec. V, with the two levels in the transport window, $\varepsilon_1, \varepsilon_2 > \mu$.

(cf. Fig. 7). In this particular case, quantum interference effects may be important[52] depending on the concrete geometry of the system. However, in the weak-coupling and high-frequency limit case considered here, $\varepsilon_2 - \varepsilon_1 \gg \Gamma_{L,R}$, they can be disregarded. Contrary to the previous regimes, the contribution of the empty state,

$$\rho_0 = \frac{\Gamma_R}{2\Gamma_L+\Gamma_R}, \quad (54)$$

plays an important role here. It strongly affects the sub-Poissonian character of the photonic noise. Since the tunneling rates are considered independent of the energy, electronic transport does not depend on the level that the electron occupies when tunneling through the QD. Then, the transport characteristics (electronic current and noise) are independent of the field intensity, detuning, and the spontaneous emission,

$$I_e = \frac{2\Gamma_L\Gamma_R}{2\Gamma_L+\Gamma_R}, \quad (55)$$

$$F_e = \frac{4\Gamma_L^2+\Gamma_R^2}{(2\Gamma_L+\Gamma_R)^2}. \quad (56)$$

This case is similar to the single resonant level with a factor 2 in the tunneling from the collector, reflecting that an electron in the left lead finds two different possibilities before tunneling into the QD. Similarly to the single resonant level, the Fano factor is sub-Poissonian. However, the contribution of the two levels increases the noise. The normalized third cumulant becomes (see Appendix C)

$$\eta_e = 1 - \frac{12\Gamma_L\Gamma_R(4\Gamma_L^2+\Gamma_R^2)}{(2\Gamma_L+\Gamma_R)^4}. \quad (57)$$

Interestingly, the two resonant-level statistics coincides with the single resonant one when writing $\Gamma_L/2$ for Γ_L. That is not the case for the photonic statistics, which depends on the population of the upper level and, therefore, on the ac field parameters. For instance, the photonic current is

$$I_p = \frac{\gamma\Gamma_L[2\Omega^2+\Gamma_R(\gamma+2\Gamma_R)]}{(2\Gamma_L+\Gamma_R)(\gamma^2+2\Omega^2+3\gamma\Gamma_R+2\Gamma_R^2)}. \quad (58)$$

The expressions for the second-order moments are quite lengthy, unless one considers a simpler case, where the tunneling rates are the same through both barriers, $\Gamma_L = \Gamma_R = \Gamma$. Then, one obtains a sub-Poissonian Fano factor,

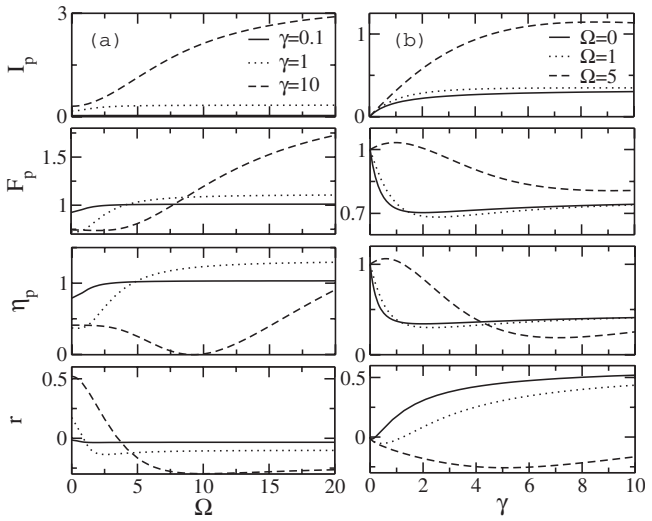

FIG. 8. $\varepsilon_1, \varepsilon_2 > \mu$: dependence of the photonic current, Fano factor, and skewness and the electron-photon correlation coefficient on (a) the field intensity, Ω, for different photon emission rates and (b) the photon emission rate, γ, for different field intensities for $\mu < \varepsilon_{1,2}$. $\Gamma_L = \Gamma_R = \Gamma = 1$. The electronic statistics (not shown) is sub-Poissonian and not affected by the ac field or by photonic relaxation. The electron-photon correlation coefficient is positive if $\gamma > \Gamma$.

$$F_p = 1 - \frac{2\gamma}{9\Gamma[2\Omega^2 + (\gamma+\Gamma)(\gamma+2\Gamma)]^2}[\Gamma(\gamma+2\Gamma)^2(\gamma+4\Gamma) + (14\Gamma^2 + 17\Gamma\gamma - \gamma^2)\Omega^2 - 2\Omega^4], \tag{59}$$

which can be tuned to super-Poissonian for high enough intensities. The electron-photon correlation, obtained from Eq. (C2), may be positive or negative depending on the concrete parametrization of the system, as discussed below. In concrete, positive correlation is obtained when $\Gamma_L \ll \Gamma_R$ as well as, for low intensity driving, when the tunneling rates are small compared to the photon emission rate (cf. Fig. 8).

A. Undriven case: $\Omega = 0$

The emission of a photon, in this case, depends on the tunneling of an electron from the left lead to the upper level. Then, it can tunnel to the collector directly or after being relaxed to the lower level by the emission of one photon. Therefore, photons *adopt* the electronic sub-Poissonian statistics,

$$F_p = 1 - \frac{2\gamma\Gamma_L\Gamma_R(\gamma + 2\Gamma_L + 2\Gamma_R)}{(\gamma+\Gamma_R)^2(2\Gamma_L+\Gamma_R)^2}, \tag{60}$$

which is maintained for all the low ac intensity regimes, and the resonance fluorescencelike behavior is completely lost (cf. Fig. 8).

The sign of the electron-photon correlation depends on the asymmetry of the tunneling couplings. Concretely, in the case $\gamma \ll \Gamma_R$, it is positive if $\Gamma_L < \frac{\Gamma_R^2}{2\gamma}$, also if the photon emission rate is large enough compared to the tunneling rates. Concretely once an electron occupies the upper level, it will rather be relaxed to the lower level and tunnel to the collector than directly tunnel from the upper level. Then, the probability of detecting consequently one photon and one electron increases, thus making the electron-photon correlation positive if

$$\gamma > \frac{\Gamma_R^2(2\Gamma_L - \Gamma_R)}{4\Gamma_L^2 + \Gamma_R^2}. \tag{61}$$

This is more clearly seen when considering $\Gamma_L = \Gamma_R = \Gamma$,

$$r = (5\gamma - \Gamma)\sqrt{\frac{\gamma}{10(\gamma+\Gamma)(7\gamma^2 + 10\gamma\Gamma + 9\Gamma^2)}}. \tag{62}$$

The coefficient

$$\eta_p = 1 - \frac{2\gamma(7\gamma^3 + 41\Gamma\gamma^2 + 52\Gamma^2\gamma + 36\Gamma^3)}{27(\gamma+\Gamma)^4} \tag{63}$$

also shows sub-Poissonian behavior.

B. High intensity limit: $\Omega \to \infty$

For high ac field intensities, the contribution of the chemical potential of the collector is only reflected in the occupation probabilities. Particularly important for the photonic dynamics is the probability of finding the QD in its empty and lower states, since it limits photon emission. The current, in this case, is

$$I_p = \frac{\gamma\Gamma_L}{2\Gamma_L + \Gamma_R}. \tag{64}$$

As seen in the previous regimes, the occupation of the empty state affects the sub-Poissonian statistics (expected for resonance fluorescence) by turning it to super-Poissonian values,

$$F_p = 1 + \frac{\gamma\Gamma_R}{(2\Gamma_L + \Gamma_R)^2}. \tag{65}$$

Comparing to Eqs. (31) and (50), the higher *unoccupation* of the QD involves a higher super-Poissonian character in the photonic statistics.

High intensities allow the emission of several photons before the electron is extracted to the collector. Also, an electron tunneling from the emitter to the upper level can be extracted to the collector from the lower level without the emission of a photon. Then, the electron-photon correlation tends to be negative. However, if Γ_L is small, $\rho_0 \approx 1 - 2\Gamma_L/\Gamma_R \gg \rho_1, \rho_2$, i.e., the probability of finding the QD empty is almost one. Then, the detection of photons and electrons is restricted to short lapses of time, which makes the electron-photon correlation positive,

$$r = \frac{(\Gamma_R - 2\Gamma_L)\sqrt{\gamma\Gamma_R}}{\sqrt{2(4\Gamma_L^2 + \Gamma_R^2)[4\Gamma_L^2 + 4\Gamma_R\Gamma_L + \Gamma_R(\gamma+\Gamma_R)]}}. \tag{66}$$

The third order coefficient gives

$$\eta_p = 1 + \frac{3\gamma\Gamma_R[8\Gamma_L^2 - 2(\gamma - 4\Gamma_R)\Gamma_L + \Gamma_R(\gamma + 2\Gamma_R)]}{2(2\Gamma_L + \Gamma_R)^4}. \tag{67}$$

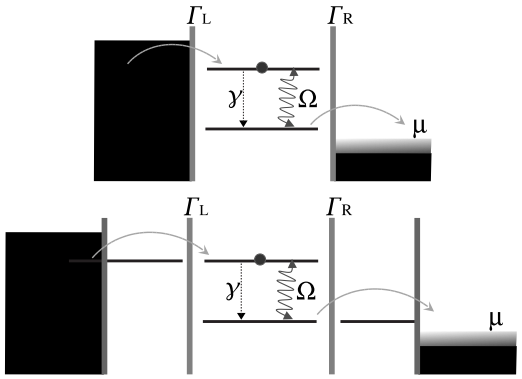

FIG. 9. Diagrams of the *selective tunneling* configuration, where each level is coupled to a different lead. *Up*: the particular system considered here. *Bottom*: a possible physical realization by considering a triple quantum dot where the lateral ones are strongly coupled to the leads so they behave as zero-dimensional leads.

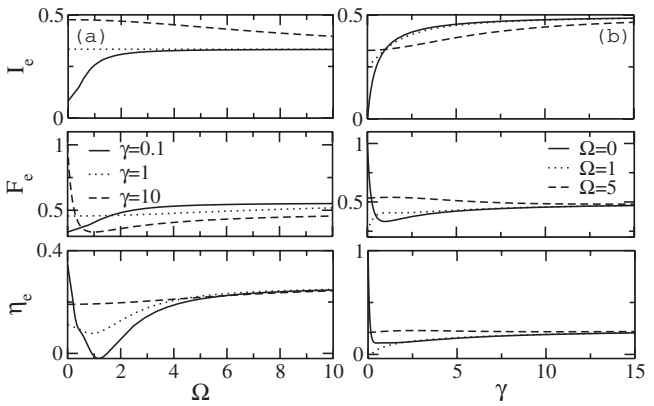

FIG. 10. Selective tunneling: electronic current, Fano factor, and skewness as a function of (a) the driving intensity for different photon emission rates and (b) the photon emission rate for different field intensities. $\Gamma_L=\Gamma_R=\Gamma=1$.

VI. SELECTIVE TUNNELING CONFIGURATION

A particularly interesting configuration in the high bias regime ($f_1=f_2=0$) where the electron-photon correlation is paradigmatic, needs *unusual* coupling to the leads: electrons can enter only to the upper level and tunnel out only from the lower one. That is, $\Gamma_{2L}=\Gamma_{1R}=\Gamma$ and $\Gamma_{1L}=\Gamma_{2R}=0$ (cf. left diagram in Fig. 9). This selective coupling to the leads could be obtained by *zero-dimensional contacts* consisting in neighbor single-level QDs strongly coupled to the leads.[53] Then, if the level of the left (right) dot is resonant with the upper (lower) level, the emitter (collector) will be uncoupled of the lower (upper) level (see lower diagram in Fig. 9). Any eventual coherence between the central dot and the lateral ones is assumed to be rapidly damped by the coupling to the leads. We note here that such a system can also be used to modulate non-Markovian dynamics by tuning the strength of the coupling of the lateral dots to the leads.

A. Undriven case: Electron-photon identification

In the absence of driving field, an electron that enters the upper level can only be transferred to the collector after being relaxed by the emission of one photon. Therefore, the electronic and photonic statistics are completely identical and $c_{i0}=c_{0i}$. This configuration is analogous of having two single-level quantum dots which are incoherently coupled, giving sub-Poissonian Fano factors[54] and maximal electron-photon correlation (see Appendix D),

$$I_e = I_p = \frac{\gamma\Gamma_L\Gamma_R}{\gamma\Gamma_L + \gamma\Gamma_R + \Gamma_L\Gamma_R}, \tag{68}$$

$$F_e = F_p = 1 - \frac{2\gamma\Gamma_L\Gamma_R(\gamma+\Gamma_L+\Gamma_R)}{[\gamma\Gamma_R+\Gamma_L(\gamma+\Gamma_R)]^2}, \tag{69}$$

$$r = 1. \tag{70}$$

The third cumulants give, for $\Gamma_L=\Gamma_R=\Gamma$,

$$\eta_e = \eta_p = 1 - 6\gamma\frac{(3\gamma^2+\Gamma^2)\Gamma + (\gamma+\Gamma)[2\gamma^2+\Gamma(\gamma+\Gamma)]}{(2\gamma+\Gamma)^4}. \tag{71}$$

B. Driven case

The ac field allows the tunneling of an electron to the collector without having previously emitted a photon as well as the emission of several photons from the relaxation of the same electron. This makes the electronic and photonic currents differ, thus uncorrelating the electronic and photonic statistics. More interestingly, by looking at the dependence of the electronic and photonic currents with the detuning,

$$I_e = \frac{\Gamma_L\Gamma_R[4\gamma\Delta_\omega^2 + (\gamma+\Gamma_R)(\gamma^2+\Gamma_R\gamma+\Omega^2)]}{\Gamma_L(\gamma+\Gamma_R)(\gamma^2+2\Gamma_R\gamma+2\Omega^2+\Gamma_R^2+4\Delta_\omega^2) + \Gamma_R[4\gamma\Delta_\omega^2+(\gamma+\Gamma_R)(\gamma^2+\Gamma_R\gamma+\Omega^2)]}, \tag{72}$$

$$I_p = \frac{\gamma\Gamma_L\{4\Gamma_R\Delta_\omega^2 + (\gamma+\Gamma_R)[\Omega^2+\Gamma_R(\gamma+\Gamma_R)]\}}{\Gamma_L(\gamma+\Gamma_R)(\gamma^2+2\Gamma_R\gamma+2\Omega^2+\Gamma_R^2+4\Delta_\omega^2) + \Gamma_R[4\gamma\Delta_\omega^2+(\gamma+\Gamma_R)(\gamma^2+\Gamma_R\gamma+\Omega^2)]}, \tag{73}$$

it can be seen that their second-order derivative obeys

$$\frac{\partial^2 I_{e(p)}}{\partial \Delta_\omega^2} \propto \Gamma_R - \gamma, \tag{74}$$

which is reflected in a resonance to antiresonance crossover. As a consequence, one can extract information on the sample-depending spontaneous photon emission rate, γ, by externally modifying the tunneling couplings to the collector.[55] The system, in this case, behaves as a *photon emission rate probe*.

Considering $\Gamma_L=\Gamma_R=\Gamma$, for simplicity, and the resonance condition, $\Delta_\omega=0$, we obtain for the Fano factors

$$F_e = 1 - \frac{2(\gamma^4 + 4\Gamma\gamma^3 + 5\Gamma^2\gamma^2 + 3\Omega^2\gamma^2 + 2\Gamma^3\gamma + 3\Gamma\Omega^2\gamma + 2\Omega^4 + 4\Gamma^2\Omega^2)}{(2\gamma^2 + 3\Gamma\gamma + \Gamma^2 + 3\Omega^2)^2}, \tag{75}$$

$$F_p = 1 - \frac{2\gamma[2\Gamma^4 - \Omega^2\Gamma^2 + \gamma^3\Gamma - \Omega^4 + \gamma^2(4\Gamma^2 - \Omega^2) + \gamma(5\Gamma^3 + 6\Omega^2\Gamma)]}{\Gamma(2\gamma^2 + 3\Gamma\gamma + \Gamma^2 + 3\Omega^2)^2}, \tag{76}$$

(cf. Figs. 10 and 13). From the Fano factor, it can be seen that the electrons obey sub-Poissonian statistics while the photons become super-Poissonian for high enough field intensities. The driving field also contributes to make the electron-photon correlation coefficient negative (see Appendix D).

In the absence of relaxation, this configuration can be mapped into a coherently coupled single-level double quantum dot, where interdot hopping played the role of the ac driving (within the rotating wave approximation). Then, in the particular case where $\Gamma_R<\Gamma_L$, the noise is sub-Poissonian in resonance, having two super-Poissonian peaks in its vicinity, when the influence of photons is small, as seen in Fig. 11. For $\gamma=0$,[56]

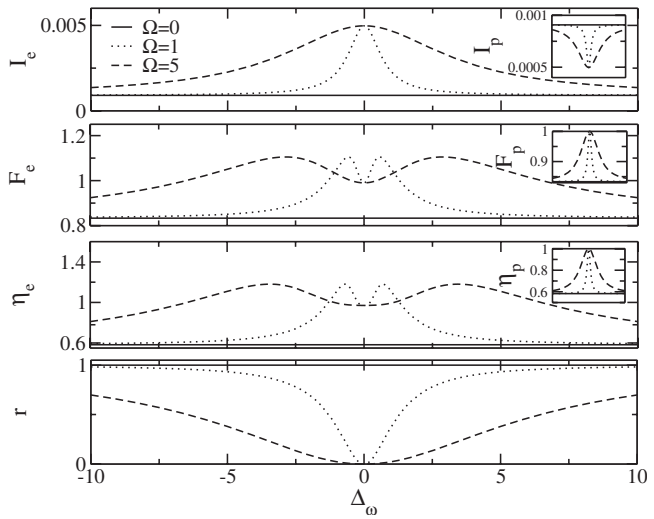

FIG. 11. Selective tunneling: electronic current, Fano factor, skewness, and electron-photon correlation as functions of the frequency detuning for different field intensities. $\Gamma_L=1$, $\Gamma_R=0.001$, and $\gamma=0.001$. In the insets the corresponding photonic values are shown. When the photon emission rate is much smaller than the tunneling rates and $\Gamma_L>\Gamma_R$, the system behaves as a coherently coupled double quantum dot, showing a sub-Poissonian minimum in the Fano factor which is between two super-Poissonian peaks.

$$F_e = 1 - \frac{2\Omega^2\Gamma_L[4(\Gamma_R - \Gamma_L)\Delta_\omega^2 + \Gamma_R(2\Omega^2 + \Gamma_R^2 + 3\Gamma_L\Gamma_R)]}{[\Gamma_R\Omega^2 + \Gamma_L(2\Omega^2 + \Gamma_R^2 + 4\Delta_\omega^2)]^2}. \tag{77}$$

This kind of features has been the subject of recent works in double quantum dot systems where the double peak structure in the electronic Fano factor becomes asymmetric by the effect of temperature.[36,57] In our case, the level energies are not shifted, so the contribution of photon emission is constant all over the ac frequency tuning and the double peak remains symmetric. As a consequence, transport is not quenched by detuning and electronic noise is sub-Poissonian far from resonance (where the ac field has no effect on transport), as expected from Eq. (69). Interestingly, the maximal

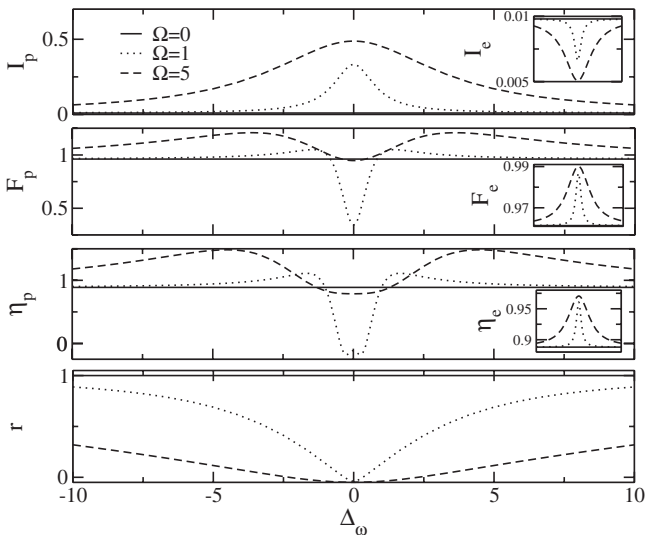

FIG. 12. Selective tunneling: photonic current, Fano factor, skewness, and electron-photon correlation as functions of the frequency detuning for different field intensities. $\Gamma_L=\gamma=1$ and $\Gamma_R=0.001$. The insets show the electronic correspondents. The double peak in the electronic Fano factor seen in Fig. 11 is washed out by a larger photon emission rate.

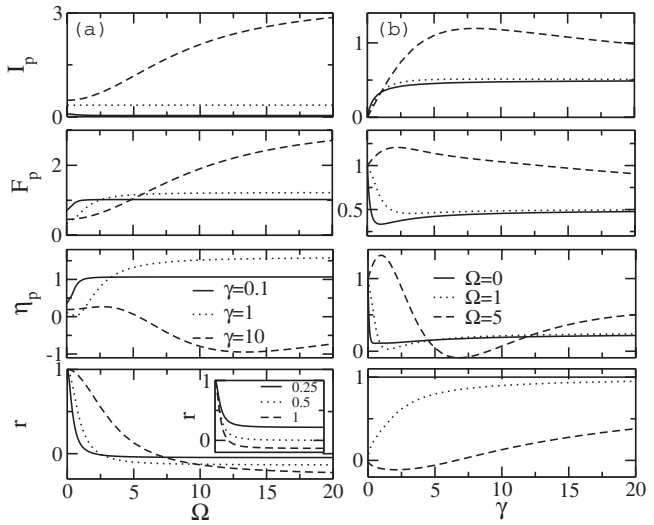

FIG. 13. Selective tunneling: photonic current, Fano factor, and skewness as a function of (a) the driving intensity for different photon emission rates and (b) the photon emission rate for different field intensities. $\Gamma_L=\Gamma_R=\Gamma=1$. Inset: electron-photon correlation coefficient as a function of the field intensity for different couplings to the left contact, Γ_L, with $\Gamma_R=\gamma=1$. It is possible to tune the sign of the electron-photon correlation by means of the tunneling coupling asymmetry.

electron-photon correlation observed far from resonance vanishes for $\Delta_\omega=0$.

The double peak in the electronic Fano factor is washed out for larger photon emission rates, even for the case $\Gamma_L \gg \Gamma_R$,

$$F_e = 1 - \frac{2\Gamma_R}{\gamma}\left[1 - \frac{(5\gamma^2 + 4\Omega^2 + 4\Delta_\omega^2)\Omega^2}{(\gamma^2 + 2\Omega^2 + 4\Delta_\omega^2)^2} + \frac{\gamma}{\Gamma_L}\left(1 - \frac{\Omega^2}{\gamma^2 + 2\Omega^2 + 4\Delta_\omega^2}\right)\right] + O(\Gamma_R^2), \quad (78)$$

as seen in the insets of Fig. 12. On contrary, in this regime, it is the photonic noise which is sub-Poissonian but for two super-Poissonian regions around the resonant frequency, recovering the resonance fluorescence behavior (see Fig. 12).

C. High intensity limit: $\Omega \to \infty$

An intense driving involves the delocalization of the electron between the upper and lower levels, so it has the same probability of occupying each of them: $\rho_1=\rho_2=\Gamma_L/(2\Gamma_L+\Gamma_R)$. In this case, the resonant currents are

$$\frac{I_e}{\Gamma_L\Gamma_R} = \frac{I_p}{\gamma\Gamma_L} = \frac{1}{2\Gamma_L + \Gamma_R}. \quad (79)$$

The electronic dynamics becomes independent of photon emission so the Fano factor coincides with that obtained for transport through a double quantum dot in the absence of dissipation, being sub-Poissonian at resonance ($\Delta_\omega=0$),

$$F_e = 1 - \frac{4\Gamma_L\Gamma_R}{(2\Gamma_L + \Gamma_R)^2}, \quad (80)$$

and super-Poissonian close to resonance if $\Gamma_L > \Gamma_R$.[36,57]

The high probability of finding the QD empty, $\rho_0=\Gamma_R/(2\Gamma_L+\Gamma_R)$, kills the *resonance fluorescencelike* photon antibunching and the photonic statistics become super-Poissonian,

$$F_p = 1 + \frac{2\gamma\Gamma_R}{(2\Gamma_L + \Gamma_R)^2}. \quad (81)$$

As discussed in Secs. III–V, the electron-photon correlation is lost by the influence of the ac field. However, if the coupling to the leads is asymmetric and $\Gamma_R > 2\Gamma_L$, once the electron has tunneled out to the collector, the QD remains empty for a long period of time (compared to the lapse of time that it spends occupied). Then, the detection of electrons and photons is restricted to the short periods of time, so r remains positive [cf. inset of Fig. 13(a)],

$$r = \frac{\sqrt{\gamma\Gamma_R}(\Gamma_R - 2\Gamma_L)}{\sqrt{(4\Gamma_L^2 + \Gamma_R^2)[4\Gamma_L^2 + 4\Gamma_R\Gamma_L + \Gamma_R(2\gamma + \Gamma_R)]}}. \quad (82)$$

The third order cumulants give

$$\eta_e = 1 - \frac{12\Gamma_L\Gamma_R(4\Gamma_L^2 + \Gamma_R^2)}{(2\Gamma_L + \Gamma_R)^4} \quad (83)$$

for electrons and

$$\eta_p = 1 + \frac{6\gamma\Gamma_R[4\Gamma_L^2 - 2(\gamma - 2\Gamma_R)\Gamma_L + \Gamma_R(\gamma + \Gamma_R)]}{(2\Gamma_L + \Gamma_R)^4} \quad (84)$$

for photons.

VII. LEVEL-DEPENDENT TUNNELING

If the left and right barriers are equal, the tunneling events may differ depending on which level participates. This can be due to the concrete orbital distribution of each level. Then, one has $V_{Li}=V_{Ri}$ for the couplings in Eq. (1) and electronic transport can be parametrized, if both levels are within the transport window, by the tunneling rates $\Gamma_2=2\pi d_l|V_{l2}|^2$ and $\Gamma_1=2\pi d_l|V_{l1}|^2$ when the electron tunnels to or from the upper or the lower level, respectively, through any barrier l.[58]

The equations of motion for the generating function, $\dot{G}(t,s_e,s_p)=M(s_e,s_p)G(t,s_e,s_p)$, and the density matrix, $\dot{\rho}(t)=M(1,1)\rho(t)$ (after setting $s_e=s_p=1$), are then given by the matrix

$$M(s_e,s_p)=\begin{pmatrix} -\Gamma_2-\Gamma_1 & s_e\Gamma_1 & 0 & 0 & s_e\Gamma_2 \\ \Gamma_1 & -\Gamma_1 & i\frac{\Omega}{2} & -i\frac{\Omega}{2} & s_p\gamma \\ 0 & i\frac{\Omega}{2} & \Lambda_{12}+i\Delta_\omega & 0 & -i\frac{\Omega}{2} \\ 0 & -i\frac{\Omega}{2} & 0 & \Lambda_{12}-i\Delta_\omega & i\frac{\Omega}{2} \\ \Gamma_2 & 0 & -i\frac{\Omega}{2} & i\frac{\Omega}{2} & -\gamma-\Gamma_2 \end{pmatrix} \tag{85}$$

in the same matrix form chosen to write Eq. (8). In this case, the decoherence term is given by $\Lambda_{12}=-\frac{\Gamma_2+\Gamma_1+\gamma}{2}$.

The dependence on the level which is occupied introduces the effect of the driving field and photon emission in the electronic current even in the high bias regime. If, for instance, $\Gamma_1<\Gamma_2$, photon emission will contribute to decrease the flow of electrons. The electronic and photonic currents are, in the general case,

$$I_e=\frac{(\Gamma_2+\Gamma_1)[(\Gamma_2+\Gamma_1)(\Gamma_2\Gamma_1+\Omega^2)+\gamma\Gamma_1(\gamma+\Gamma_1+2\Gamma_2)]}{(\gamma+3\Gamma_1)\Gamma_2^2+[\gamma^2+3\Omega^2+3\Gamma_1(2\gamma+\Gamma_1)]\Gamma_2+\Gamma_1(2\gamma^2+2\Gamma_1\gamma+3\Omega^2)}, \tag{86}$$

$$I_p=\frac{\gamma[(\Gamma_2+\Gamma_1)(\Gamma_2\Gamma_1+\Omega^2)+\gamma\Gamma_2]}{(\gamma+3\Gamma_1)\Gamma_2^2+[\gamma^2+3\Omega^2+3\Gamma_1(2\gamma+\Gamma_1)]\Gamma_2+\Gamma_1(2\gamma^2+2\Gamma_1\gamma+3\Omega^2)}. \tag{87}$$

As expected, if $\Gamma_1<\Gamma_2$, the emission of photons inhibits electronic transport. However, the opposite is not true: if $\Gamma_2<\Gamma_1$, electrons will rather tunnel through the lower level, thus avoiding photon emission. These two limiting cases will be further analyzed below. In the case $\Gamma_1=\Gamma_2$, the electronic current is independent of both the relaxation rate and the driving intensity, recovering the behavior described in Sec. V (cf. Fig. 8).

A. Undriven case

In the absence of the driving field, the electronic and photonic currents are given by

$$\frac{I_e}{\Gamma_1(\gamma+\Gamma_2)(\Gamma_1+\Gamma_2)}=\frac{I_p}{\gamma\Gamma_1\Gamma_2}=\frac{1}{2\gamma\Gamma_1+(\gamma+3\Gamma_1)\Gamma_2}. \tag{88}$$

In this case, the difference in the tunneling rates of each level is enough to define the sub- or super-Poissonian electronic statistics,

$$F_e=1+\frac{2\Gamma_2(\Gamma_1^3+\tilde{\Gamma}_1\Gamma_2^2)-2\Gamma_1[\Gamma_1(\gamma+2\Gamma_2)^2+\gamma\Gamma_2\tilde{\Gamma}_2]}{[2\gamma\Gamma_1+(\gamma+3\Gamma_1)\Gamma_2]^2}, \tag{89}$$

where we have called $\tilde{\Gamma}_i=\gamma+\Gamma_i$. Interestingly, in the absence of photon relaxation, the Fano factor depends linearly on the asymmetry and increases as one of the levels becomes uncoupled of the leads (this case will be considered below),

$$F_e(\gamma\ll\Gamma_i)=1+\frac{2}{9}\left(\frac{\Gamma_1}{\Gamma_2}+\frac{\Gamma_2}{\Gamma_1}-4\right). \tag{90}$$

Photon emission diminishes this effect by contributing to make the electrons be extracted from the lower level. Then, the sub-Poissonian shot noise observed in the high bias regime [cf. Eq. (56)] is recovered,

$$F_e(\gamma\gg\Gamma_i)=1-\frac{2\Gamma_1(\Gamma_1+\Gamma_2)}{(2\Gamma_1+\Gamma_2)^2}. \tag{91}$$

On the other hand, photonic statistics remain sub-Poissonian, independently of the configuration,

$$F_p=1-\frac{2\gamma\Gamma_1\Gamma_2(\gamma+2\Gamma_1+2\Gamma_2)}{[2\gamma\Gamma_1+(\gamma+3\Gamma_1)\Gamma_2]^2}. \tag{92}$$

The electron-photon correlation coefficient (see Appendix E) shows how electrons and photons can be uncorrelated by the manipulation of the tunneling rates.

B. High intensity limit: $\Omega\to\infty$

As the driving field couples the two levels, it tends to annihilate the particular behavior introduced by the different couplings to the leads. Thus, the currents depend simply on their correspondent rate,

$$\frac{I_e}{\Gamma_1+\Gamma_2}=\frac{I_p}{\gamma}=\frac{1}{3}, \tag{93}$$

while and the electronic Fano factor and skewness become independent of the tunneling couplings: $F_e=\frac{5}{9}$ and $\eta_e=\frac{7}{27}$, consistently with Eq. (56). That is not the case for the pho-

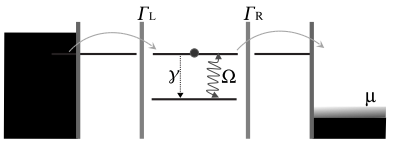

FIG. 14. Schematic diagram of the proposed setup for a level-dependent tunneling configuration where $\Gamma_1 \ll \Gamma_2$.

tonic statistics, whose second and third moments depend on the rates,

$$F_p = 1 + \frac{2\gamma}{9(\Gamma_1 + \Gamma_2)}, \tag{94}$$

$$\eta_p = 1 - \frac{2\gamma(\gamma - 9\Gamma_1 - 9\Gamma_2)}{27(\Gamma_1 + \Gamma_2)^2}. \tag{95}$$

As expected, electron-photon correlation becomes negative,

$$r = -\sqrt{\frac{\gamma}{5[2\gamma + 9(\Gamma_1 + \Gamma_2)]}}. \tag{96}$$

C. $\Gamma_1 \ll \Gamma_2$ limit

The zero-dimensional contacts introduced in Sec. VI can also be employed to simulate energy-dependent tunneling. If both zero-dimensional contacts are aligned (by tuning the gate voltages of the left and right QDs) with the same level of the QD, transport through the other level will be strongly suppressed (cf. Fig. 14). Thus, the occupation of the off resonant-level blocks the electronic current.

If the levels of the surrounding QDs are aligned with the upper level, in the absence of driving, as soon as the lower level is occupied (by the relaxation of an electron from the upper level), transport is canceled in a high bias version of dynamical channel blockade. Thus, electrons flow in bunches, while photonic transport is highly suppressed.

Again, the driving field removes the blockade, producing finite electronic and photonic currents,

$$\frac{I_e}{\Gamma_2} = \frac{I_p}{\gamma} = \frac{\Omega^2}{\gamma^2 + \gamma\Gamma_2 + 3\Omega^2}, \tag{97}$$

thus reducing the super-Poissonian electron noise,

$$F_e = 1 + 2\frac{\gamma\Gamma_2(\gamma + \Gamma_2)^2 - \Omega^2(\gamma^2 + 2\gamma\Gamma_2 - \Gamma_2^2) - 2\Omega^4}{[\gamma(\gamma + \Gamma_2) + 3\Omega^2]^2}, \tag{98}$$

which becomes sub-Poissonian for high enough driving intensities (cf. Fig. 15). This configuration resembles a single-level quantum dot coupled to a localized state, where super-Poissonian shot noise has been predicted.[59] The obtained Fano factor recovers their result for a nondissipative situation, $\gamma = 0$. Similar models were proposed to explain enhanced shot noise in single-quantum dots.[60] For low intensities, the photonic noise is sub-Poissonian, resembling the resonance fluorescence but, for $\Omega > \sqrt{2\Gamma_2(2\gamma + \Gamma_2)}$, the contribution of the empty state turns it super-Poissonian (cf. Fig. 16),

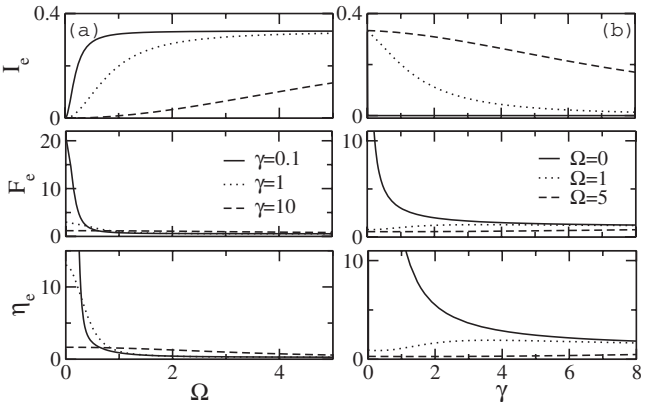

FIG. 15. Level-dependent tunneling: electronic current, Fano factor, and skewness as a function of (a) the field intensity for different photon emission rates and (b) the photon emission rate for different field intensities for the case $\Gamma_1 = 10^{-5}$ and $\Gamma_2 = 1$.

$$F_p = 1 - 2\gamma\Omega^2\frac{2\Gamma_2(2\gamma + \Gamma_2) - \Omega^2}{\Gamma_2(\gamma^2 + 3\Omega^2 + \gamma\Gamma_2)^2}. \tag{99}$$

It is interesting to note that though the electronic and photonic mean counts are proportional, their variances are not, which is reflected in the electron-photon correlation that gives $r < 1$ [see Eq. (E2)].

The undriven case gives a Fano factor that diverges when the photon emission is reduced, $F_e = 1 + 2\frac{\Gamma_2}{\gamma}$ and $\eta_e = \frac{\gamma^2 + 6\Gamma_2^2(\gamma + \Gamma_2)}{\gamma^2}$. In this case, relaxation becomes a stochastic process.

D. $\Gamma_2 \ll \Gamma_1$ limit

This case is similar to the previous one with the difference that the contribution of photon emission has the opposite

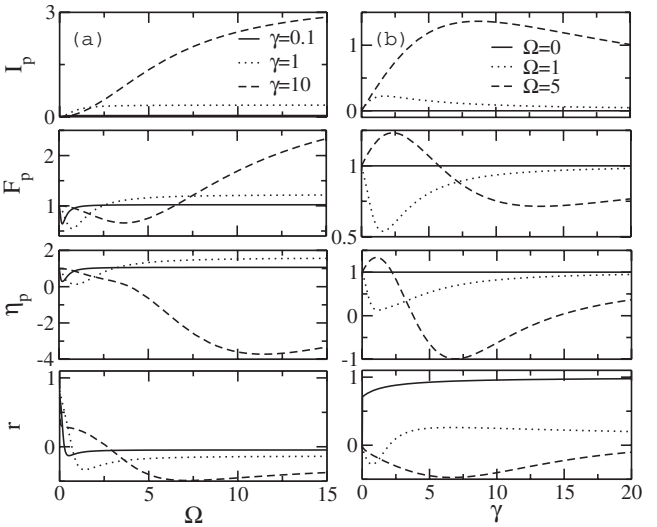

FIG. 16. Level-dependent tunneling: photonic current, Fano factor, skewness, and electron-photon correlation coefficient as a function of (a) the field intensity for different photon emission rates and (b) the photon emission rate for different field intensities for the case $\Gamma_1 = 10^{-5}$ and $\Gamma_2 = 1$.

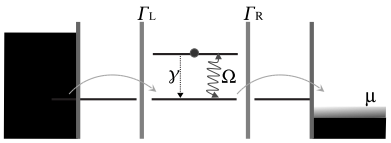

FIG. 17. Schematic diagram of the proposed setup for a level-dependent tunneling configuration where $\Gamma_2 \ll \Gamma_1$.

effect: the upper level is very weakly coupled to the leads so its population quenches the electronic current (cf. Fig. 17). Therefore, relaxation by photon emission contributes to unblock the electronic transport.

In the absence of driving, the electrons tend to be transferred through the lower level (and the system is reduced to the single resonant-level configuration[48]), so there is no chance for photon emission. The introduction of the driving field populates the upper level thus reducing the electronic current (cf. Fig. 18) and giving a finite probability to photons to be emitted—thus acting as a *photon pump* [cf. Fig. 19(a)],

$$I_e = \frac{\Gamma_1(\gamma^2 + \gamma\Gamma_1 + \Omega^2)}{2\gamma^2 + 2\gamma\Gamma_1 + 3\Omega^2}, \tag{100}$$

$$I_p = \frac{\gamma\Omega^2}{2\gamma^2 + 2\gamma\Gamma_1 + 3\Omega^2}. \tag{101}$$

The ac field modifies the electronic Fano factor typical from the single resonant level, $F_e = 1/2$, without changing its sub-Poissonian character but for the range $\Gamma_1 > \sqrt{2}\Omega \gg \gamma$,

$$F_e = 1 - \frac{2[\gamma^2(\gamma+\Gamma_1)^2 + \Omega^2(3\gamma^2 - \Gamma_1^2) + 2\Omega^4]}{(2\gamma^2 + 2\Gamma_1\gamma + 3\Omega^2)^2}. \tag{102}$$

The photonic Fano factor,

$$F_p = 1 + \frac{2\gamma\Omega^2(\gamma^2 - 5\Gamma_1\gamma - 2\Gamma_1^2 + \Omega^2)}{\Gamma_1(2\gamma^2 + 2\Gamma_1\gamma + 3\Omega^2)^2}, \tag{103}$$

can be turned from sub-Poissonian to super-Poissonian by increasing the field intensity if $\Gamma_1 > \frac{1}{2}(\sqrt{33}+5)\gamma$. Otherwise, it will be always super-Poissonian. The electron-photon correlation, calculated from Eq. (E2), is always negative.

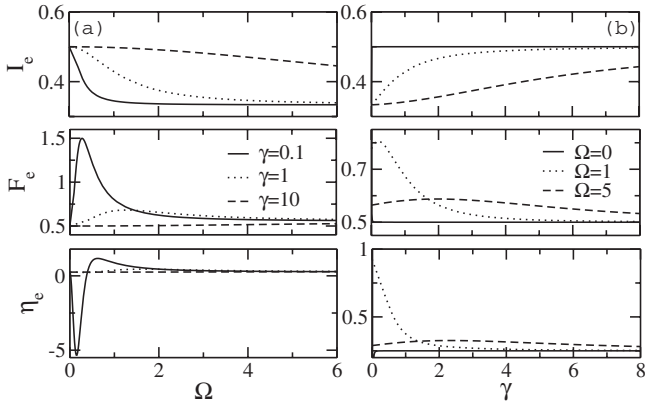

FIG. 18. Level-dependent tunneling: electronic current, Fano factor, and skewness as a function of (a) the field intensity for different photon emission rates and (b) the photon emission rate for different field intensities for the case $\Gamma_1 = 1$ and $\Gamma_2 = 10^{-5}$.

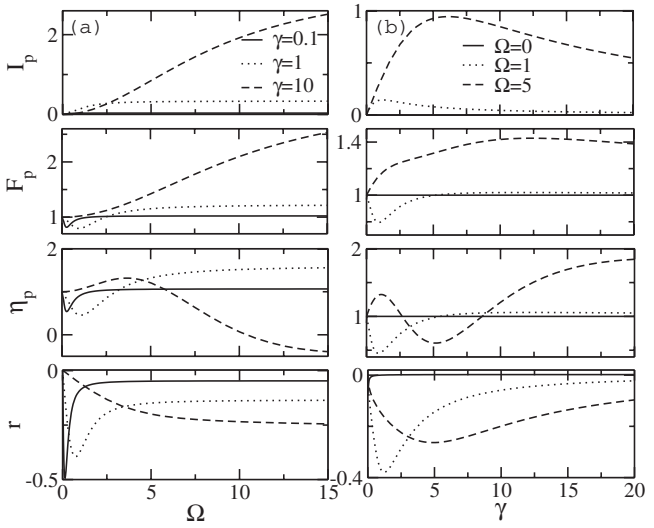

FIG. 19. Level-dependent tunneling: Photonic current, Fano factor, skewness, and electron-photon correlation coefficient as a function of (a) the field intensity for different photon emission rates and (b) the photon emission rate for different field intensities for the case $\Gamma_1 = 1$ and $\Gamma_2 = 10^{-5}$.

The third electronic cumulant varies between $\eta_e = \frac{1}{4}$ for $\Omega = 0$ and $\eta_e = \frac{7}{27}$ for the high intensity limit, but it shows a deep minimum for low voltages where it is negative (cf. Fig. 18). The photonic one is removed by the ac field from $\eta_p = 1$ to the asymptotic limit,

$$\eta_p = 1 - \frac{2\gamma(\gamma - 9\Gamma_1)}{27\Gamma_1^2}, \tag{104}$$

for $\Omega \to \infty$. Then, the skewness of the photonic statistics can be tuned by the strength of the tunneling couplings.

VIII. CONCLUSIONS

A method for extracting the simultaneous counting statistics for electrons tunneling through an ac driven two-level quantum dot and for photons emitted in the intradot electron relaxation processes is presented. It allows us to calculate all the electronic and photonic cumulants as well as the correlation between fermionic and bosonic statistics, showing how they affect each other. For instance, photon emission is shown to reduce the super-Poissonian electronic shot noise in the dynamical channel blockade regime. On the other hand, a purely quantum feature as is sub-Poissonian statistics in a two-level photon source (resonance fluorescence) is lost as the electron is allowed to escape from the system. Our method can be applied to obtain the correlations between processes of different kinds affecting to the same system as could be spin dependent transport or three terminal devices.

It is shown how the character of the electronic and photonic fluctuations can be manipulated by tuning the external parameters such as the intensity of the ac field, the chemical potential of the right lead, or the tunneling barriers. By this kind of measurements, information about electron relaxation

times can be obtained. All the combinations of sub- and super-Poissonian noises can be selected in this way.[37]

We present an analysis of the electron-photon correlations which gives a more complete understanding of the dynamical behavior of each concrete sample configuration and the importance of relaxation processes in transport properties. In this sense, a configuration with a maximal electron-photon correlation is proposed. Additionally, this configuration can serve as a probe for the photonic emission rate.

A triple quantum dot system is proposed in order to control tunneling through the central two-level quantum dot, while the levels of the neighbor dots act as zero-dimensional leads. This way, assorted configurations which can be mapped to coherently or incoherently coupled double quantum dot systems or quantum dots coupled to localized states can be achieved, providing a way to explore the effect of coherence in electronic transport.

ACKNOWLEDGMENTS

We thank M. Büttiker for comments. R.S. and G.P. were supported by the M.E.C. of Spain through Grant No. MAT2005-00644. T.B. acknowledges support by the German DFG under Project No. BR 1528/5-1 and the DAAD.

APPENDIX A: PHOTONIC RESONANCE FLUORESCENCE

When the chemical potential is above the energies of both levels, so the probability for an electron in the upper level to tunnel to the collector is $x\Gamma_R$, the up to second-order moments are given by the coefficients (considering the Taylor expansion around $x=0$)

$$c_{20} = -\frac{\Omega^2\Gamma_L^2\Gamma_R^2[\Omega^2(\gamma^2+2\Omega^2)-\gamma(\gamma-2\Omega)(\gamma+2\Omega)(\Gamma_L+\Gamma_R)]}{2[(\gamma^2+2\Omega^2)^3(\Gamma_L+\Gamma_R)^3]}x^2+O(x^3), \tag{A1}$$

$$c_{02} = -\frac{3\gamma^3\Omega^4}{(\gamma^2+2\Omega^2)^3}-\frac{\gamma^2\Omega^4\Gamma_R}{(\gamma^2+2\Omega^2)^3}\left(\frac{\gamma(\gamma^2-16\Omega^2)}{4(\gamma^2+2\Omega^2)(\Gamma_L+\Gamma_R)}-\frac{\Omega^2}{4(\Gamma_L+\Gamma_R)^2}-\frac{23\gamma^2-8\Omega^2}{2(\gamma^2+2\Omega^2)}\right)x+O(x^2), \tag{A2}$$

$$c_{11} = \frac{\gamma\Omega^2\Gamma_L\Gamma_R[\gamma(\gamma^2-10\Omega^2)(\Gamma_L+\Gamma_R)-\Omega^2(\gamma^2+2\Omega^2)]}{2(\gamma^2+2\Omega^2)^3(\Gamma_L+\Gamma_R)^2}x+O(x^2). \tag{A3}$$

For the undriven and high ac intensity limits, one can give short expressions without having to do the Taylor expansion around $x=0$. In the undriven case, $\Omega=0$, the electron-photon correlation is given by

$$c_{11} = \frac{c_{01}[x\Gamma_L\Gamma_R-2c_{10}(\gamma+2\Gamma_L+2\Gamma_R)]}{\Gamma_L(2\gamma+x\Gamma_R)+\Gamma_R[x\Gamma_R-(x-2)\gamma]}-\frac{8c_{10}c_{01}}{\gamma+x\Gamma_R}. \tag{A4}$$

In the opposite case, $\Omega\to\infty$ obtains the electron-photon correlation from the coefficient

$$c_{11} = \frac{4xc_p\Gamma_L\Gamma_R+c_e\{(\gamma-4c_p)(\gamma+4\Gamma_L)-[(x-4)\gamma+16c_p]\Gamma_R\}}{[4\Gamma_L-(x-4)\Gamma_R](\gamma+x\Gamma_R)} \tag{A5}$$

and the skewness of the electronic and photonic statistics from

$$c_{30} = \frac{64x^3\Gamma_L^3\Gamma_R^3}{[4\Gamma_L+(4-x)\Gamma_R]^5}, \tag{A6}$$

$$c_{03} = -\frac{x\gamma^3\Gamma_R[4\Gamma_L+(4-3x)\Gamma_R][2\Gamma_L+(2-x)\Gamma_R]}{[4\Gamma_L+(4-x)\Gamma_R]^5}. \tag{A7}$$

APPENDIX B: DYNAMICAL CHANNEL BLOCKADE REGIME

If the chemical potential of the collector is between the energies of each level, so the occupation of the lower level avoids electrons from tunneling through the upper one, until it is extracted with a rate $x\Gamma_R$; the second-order correlations are given by (considering $x=0$)

$$\begin{aligned} c_{20} = {} & c_{10}\frac{\Gamma_L\Gamma_R(\gamma^2+2\Gamma_R\gamma+4\Omega^2+\Gamma_R^2)}{(\gamma+\Gamma_R)[\Gamma_R(\gamma^2+2\Gamma_R\gamma+3\Omega^2+\Gamma_R^2)+\Gamma_L(2\gamma^2+3\Gamma_R\gamma+4\Omega^2+\Gamma_R^2)]} \\ & -c_{10}^2\frac{\gamma^3+2\Omega^2\gamma+13\Gamma_R^2\gamma+6\Gamma_R^3+8(\gamma^2+\Omega^2)\Gamma_R+2\Gamma_L(5\gamma^2+8\Gamma_R\gamma+4\Omega^2+3\Gamma_R^2)}{(\gamma+\Gamma_R)[\Gamma_R(\gamma^2+2\Gamma_R\gamma+3\Omega^2+\Gamma_R^2)+\Gamma_L(2\gamma^2+3\Gamma_R\gamma+4\Omega^2+\Gamma_R^2)]}, \end{aligned} \tag{B1}$$

$$c_{02} = c_{01}\frac{\gamma\Omega^2(\gamma+4\Gamma_L+3\Gamma_R) - c_{01}[\gamma^3+2\Omega^2\gamma+13\Gamma_R^2\gamma+6\Gamma_R^3+8(\gamma^2+\Omega^2)\Gamma_R+2\Gamma_L(5\gamma^2+8\Gamma_R\gamma+4\Omega^2+3\Gamma_R^2)]}{(\gamma+\Gamma_R)[\Gamma_R(\gamma^2+2\Gamma_R\gamma+3\Omega^2+\Gamma_R^2)+\Gamma_L(2\gamma^2+3\Gamma_R\gamma+4\Omega^2+\Gamma_R^2)]}, \tag{B2}$$

$$c_{11} = \frac{-\gamma\Omega^2(\gamma+4\Gamma_L+3\Gamma_R)+c_{01}\Gamma_L\Gamma_R(\gamma^2+2\Gamma_R\gamma+4\Omega^2+\Gamma_R^2)}{(\gamma+\Gamma_R)[\Gamma_R(\gamma^2+2\Gamma_R\gamma+3\Omega^2+\Gamma_R^2)+\Gamma_L(2\gamma^2+3\Gamma_R\gamma+4\Omega^2+\Gamma_R^2)]} \tag{B3}$$

$$-c_{10}\frac{2c_{01}[\gamma^3+2\Omega^2\gamma+6\Gamma_R^3+(13\gamma+6\Gamma_L)\Gamma_R^2+2(5\gamma^2+4\Omega^2)\Gamma_L+8(\gamma^2+2\Gamma_L\gamma+\Omega^2)\Gamma_R]}{(\gamma+\Gamma_R)[\Gamma_R(\gamma^2+2\Gamma_R\gamma+3\Omega^2+\Gamma_R^2)+\Gamma_L(2\gamma^2+3\Gamma_R\gamma+4\Omega^2+\Gamma_R^2)]}. \tag{B4}$$

For small x, in the undriven configuration, $\Omega=0$, the electron-photon correlation is given by

$$c_{11} = \frac{\gamma\Gamma_L\Gamma_R(\gamma+\Gamma_R)(2\Gamma_L+\Gamma_R)x}{[\Gamma_R(\gamma+\Gamma_R)+\Gamma_L(2\gamma+\Gamma_R)]^2}+O(x^2). \tag{B5}$$

In the opposite limit, $\Omega\to\infty$, we find short expressions for the electron-photon correlation,

$$c_{11} = -\frac{2(x+1)\gamma\Gamma_L\Gamma_R[4\Gamma_L+(1-3x)\Gamma_R]}{[4\Gamma_L+(3-x)\Gamma_R]^3}, \tag{B6}$$

and the third order moments,

$$c_{30} = \frac{64(x+1)^3\Gamma_L^3\Gamma_R^3}{[4\Gamma_L+(3-x)\Gamma_R]^5}, \tag{B7}$$

$$c_{03} = -\frac{(x+1)\gamma^3\Gamma_R[8\Gamma_L^2+2(3-5x)\Gamma_R\Gamma_L+(3x^2-4x+1)\Gamma_R^2]}{[4\Gamma_L+(3-x)\Gamma_R]^5}. \tag{B8}$$

APPENDIX C: BOTH LEVELS IN THE TRANSPORT WINDOW

If the chemical potential of the collector is below the energy of both levels, the photonic shot noise and the electron-photon correlation can be obtained from

$$c_{02} = c_{01}\frac{\gamma\{(\gamma+2\Gamma_R)\Omega^2+4\Gamma_L[\Omega^2+\Gamma_R(\gamma+2\Gamma_R)]\}}{(2\Gamma_L+\Gamma_R)(\gamma+2\Gamma_R)(\gamma^2+3\Gamma_R\gamma+2\Omega^2+2\Gamma_R^2)} - c_{01}^2\frac{\gamma^3+2\Omega^2\gamma+2\Gamma_R(5\gamma^2+12\Gamma_R\gamma+4\Omega^2+8\Gamma_R^2)+2\Gamma_L[5\gamma^2+4\Omega^2+4\Gamma_R(4\gamma+3\Gamma_R)]}{(2\Gamma_L+\Gamma_R)(\gamma+2\Gamma_R)(\gamma^2+3\Gamma_R\gamma+2\Omega^2+2\Gamma_R^2)}, \tag{C1}$$

$$\begin{aligned} c_{11} = {} & \frac{1}{(2\Gamma_L+\Gamma_R)(\gamma+2\Gamma_R)(\gamma^2+3\Gamma_R\gamma+2\Omega^2+2\Gamma_R^2)}[\Gamma_L\Gamma_R\gamma(\gamma+2\Gamma_R)^2+2c_{01}\Gamma_L\Gamma_R[5\gamma^2+4\Omega^2+4\Gamma_R(4\gamma+3\Gamma_R)] \\ & +c_{10}\gamma\{(\gamma+2\Gamma_R)\Omega^2+4\Gamma_L[\Omega^2+\Gamma_R(\gamma+2\Gamma_R)]\} \\ & -2c_{10}c_{01}\{\gamma^3+2\Omega^2\gamma+2\Gamma_R(5\gamma^2+12\Gamma_R\gamma+4\Omega^2+8\Gamma_R^2)+2\Gamma_L[5\gamma^2+4\Omega^2+4\Gamma_R(4\gamma+3\Gamma_R)]\}]. \end{aligned} \tag{C2}$$

We also obtain the skewness of the photonic statistics for the undriven case, $\Omega=0$,

$$c_{03} = \frac{\gamma^3\Gamma_L^3\Gamma_R^3[2\gamma^2+8\Gamma_L^2+7\Gamma_R(\gamma+\Gamma_R)+2\Gamma_L(3\gamma+7\Gamma_R)]}{(\gamma+\Gamma_R)^5(2\Gamma_L+\Gamma_R)^5}, \tag{C3}$$

and in the high ac intensity regime,

$$c_{03} = \frac{\gamma^3\Gamma_L\Gamma_R(\Gamma_R-2\Gamma_L)}{4(2\Gamma_L+\Gamma_R)^5}. \tag{C4}$$

APPENDIX D: SELECTIVE TUNNELING CONFIGURATION

In the configuration describe in Sec. VI, the electronic and photonic correlations are given by

$$c_{20} = \frac{c_{10} 2\Gamma_L \Gamma_R (2\gamma^2 + 2\Gamma_R \gamma + \Omega^2)}{(\gamma + \Gamma_R)[\Gamma_R(\gamma^2 + \Gamma_R\gamma + \Omega^2) + \Gamma_L(\gamma^2 + 2\Gamma_R\gamma + 2\Omega^2 + \Gamma_R^2)]} - c_{10}^2 \frac{\gamma^3 + 2\Omega^2\gamma + \Gamma_R(7\gamma^2 + 7\Gamma_R\gamma + 4\Omega^2 + \Gamma_R^2) + \Gamma_L[5\gamma^2 + 4\Omega^2 + 5\Gamma_R(2\gamma + \Gamma_R)]}{(\gamma + \Gamma_R)[\Gamma_R(\gamma^2 + \Gamma_R\gamma + \Omega^2) + \Gamma_L(\gamma^2 + 2\Gamma_R\gamma + 2\Omega^2 + \Gamma_R^2)]}, \tag{D1}$$

$$c_{02} = \frac{c_{01}\gamma\{(\gamma + \Gamma_R)\Omega^2 + 2\Gamma_L[\Omega^2 + 2\Gamma_R(\gamma + \Gamma_R)]\}}{(\gamma + \Gamma_R)[\Gamma_R(\gamma^2 + \Gamma_R\gamma + \Omega^2) + \Gamma_L(\gamma^2 + 2\Gamma_R\gamma + 2\Omega^2 + \Gamma_R^2)]} - c_{01}^2 \frac{\gamma^3 + 2\Omega^2\gamma + \Gamma_R(7\gamma^2 + 7\Gamma_R\gamma + 4\Omega^2 + \Gamma_R^2) + \Gamma_L[5\gamma^2 + 4\Omega^2 + 5\Gamma_R(2\gamma + \Gamma_R)]}{(\gamma + \Gamma_R)[\Gamma_R(\gamma^2 + \Gamma_R\gamma + \Omega^2) + \Gamma_L(\gamma^2 + 2\Gamma_R\gamma + 2\Omega^2 + \Gamma_R^2)]}, \tag{D2}$$

and, considering $\Gamma_L = \Gamma_R = \Gamma$, for simplicity,

$$c_{11} = \frac{\gamma[\Gamma(\gamma + \Gamma)^3(2\gamma^2 + \Gamma^2) - \gamma(\gamma - 11\Gamma)\Gamma(\gamma + \Gamma)\Omega^2 - (\gamma^2 + \Gamma\gamma - 4\Gamma^2)\Omega^4 - \Omega^6]}{[3\Omega^2 + (\gamma + \Gamma)(2\gamma + \Gamma)]^3}. \tag{D3}$$

In the undriven case, $\Omega = 0$, the third order coefficients are

$$c_{30} = c_{03} = \gamma^3 \Gamma_L^3 \Gamma_R^3 \frac{2(\gamma^2 + \Gamma_L^2 + \Gamma_R^2) + 3(\gamma\Gamma_L + \gamma\Gamma_R + \Gamma_L\Gamma_R)}{(\gamma\Gamma_L + \gamma\Gamma_R + \Gamma_L\Gamma_R)^5}. \tag{D4}$$

APPENDIX E: LEVEL-DEPENDENT TUNNELING

The tunneling between the leads and the quantum dot may depend on the involved level of the quantum dot. We consider here the case $\Gamma_{iL} = \Gamma_{iR} = \Gamma_i$, where $i = \{1, 2\}$. In the undriven case ($\Omega = 0$), the electron-photon correlation is determined by the coefficient

$$c_{11} = \frac{\gamma\Gamma_1\Gamma_2[(\gamma - \Gamma_1)\Gamma_2^3 + (\gamma + \Gamma_1)^2\Gamma_2^2 + \Gamma_1(2\gamma^2 + 3\Gamma_1\gamma - \Gamma_1^2)\Gamma_2 + 2\gamma(\gamma - \Gamma_1)\Gamma_1^2]}{[2\gamma\Gamma_1 + (\gamma + 3\Gamma_1)\Gamma_2]^3}. \tag{E1}$$

We can give general expressions for the electron-photon correlation when tunneling though the one of the levels is suppressed. For $\Gamma_1 \ll \Gamma_2$

$$c_{11} = \gamma\Omega^2 \frac{\gamma\Gamma_2(\gamma + \Gamma_2)^2 - \Omega^2(\gamma^2 + \Gamma_2^2 + 6\gamma\Gamma_2) - \Omega^4}{(\gamma^2 + 3\Omega^2 + \gamma\Gamma_2)^3} \tag{E2}$$

and for $\Gamma_2 \ll \Gamma_1$

$$c_{11} = -\frac{\gamma\Omega^2[2\gamma\Gamma_1^3 + (8\gamma^2 + \Omega^2)\Gamma_1^2 + (6\gamma^3 + 4\Omega^2\gamma)\Gamma_1 + \Omega^2(\gamma^2 + \Omega^2)]}{(2\gamma^2 + 2\Gamma_1\gamma + 3\Omega^2)^3}. \tag{E3}$$

[1] T. Brandes, Phys. Rep. **408**, 315 (2005).

[2] H. Haug and A. P. Jauho, *Quantum Kinetics and Optics of Semiconductors* (Springer, Berlin, 1996).

[3] H. Bruus and K. Flensberg, *Many-Body Quantum Theory in Condensed Matter Physics* (Oxford University Press, Oxford, 2004).

[4] G. Platero and R. Aguado, Phys. Rep. **395**, 1 (2004).

[5] T. Brandes and B. Kramer, Phys. Rev. Lett. **83**, 3021 (1999).

[6] M. Henny, S. Oberholzer, C. Strunk, T. Heinzel, K. Ensslin, M. Holland, and C. Schönenberger, Science **284**, 296 (1999); W. D. Oliver, J. Kim, R. C. Liu, and Y. Yamamoto, *ibid.* **284**, 299 (1999).

[7] J. Kim, O. Benson, H. Kan, and Y. Yamamoto, Nature (London) **397**, 500 (1999).

[8] P. Michler, A. Kiraz, C. Becher, W. V. Schoenfeld, P. M. Petroff, L. Zhang, E. Hu, and A. Imamoğlu, Science **290**, 2282 (2000).

[9] O. Benson, C. Santori, M. Pelton, and Y. Yamamoto, Phys. Rev. Lett. **84**, 2513 (2000).

[10] J. Gabelli, L.-H. Reydellet, G. Fève, J.-M. Berroir, B. Plaçais, P. Roche, and D. C. Glattli, Phys. Rev. Lett. **93**, 056801 (2004).

[11] M. Merlo, F. Haupt, F. Cavaliere, and M. Sassetti, New J. Phys. **10**, 023008 (2008).

[12] C. W. J. Beenakker and H. Schomerus, Phys. Rev. Lett. **86**, 700 (2001).

[13] C. W. J. Beenakker and H. Schomerus, Phys. Rev. Lett. **93**, 096801 (2004).

[14] E. Arimondo and G. Orriols, Lett. Nuovo Cimento Soc. Ital. Fis. **17**, 333 (1976); G. Alzetta, A. Gozzini, L. Moi, and G. Orriols,

Nuovo Cimento Soc. Ital. Fis., B **36**, 5 (1976).
[15] H. R. Gray, R. M. Whitley, and C. R. Stroud, Jr., Opt. Lett. **3**, 218 (1978).
[16] T. Brandes and F. Renzoni, Phys. Rev. Lett. **85**, 4148 (2000).
[17] B. Michaelis, C. Emary, and C. W. J. Beenakker, Europhys. Lett. **73**, 677 (2006).
[18] M. Büttiker, Phys. Rev. B **46**, 12485 (1992).
[19] Ya. M. Blanter and M. Büttiker, Phys. Rep. **336**, 1 (2000).
[20] L. S. Levitov and G. B. Lesovik, Pis'ma Zh. Eksp. Teor. Fiz. **58**, 225 (1993) [JETP Lett. **58**, 230 (1993)].
[21] D. A. Bagrets and Yu. V. Nazarov, Phys. Rev. B **67**, 085316 (2003).
[22] F. J. Kaiser and S. Kohler, Ann. Phys. **16**, 702 (2007).
[23] R. J. Glauber, Phys. Rev. Lett. **10**, 84 (1963).
[24] P. L. Kelley and W. H. Kleiner, Phys. Rev. **136**, A316 (1964).
[25] M. O. Scully and W. E. Lamb, Jr., Phys. Rev. **179**, 368 (1969).
[26] R. J. Cook, Phys. Rev. A **23**, 1243 (1981).
[27] R. J. Cook, Opt. Commun. **35**, 347 (1980).
[28] D. Lenstra, Phys. Rev. A **26**, 3369 (1982).
[29] S. Gustavsson, R. Leturcq, B. Simovič, R. Schleser, T. Ihn, P. Studerus, K. Ensslin, D. C. Driscoll, and A. C. Gossard, Phys. Rev. Lett. **96**, 076605 (2006).
[30] S. Gustavsson, R. Leturcq, B. Simovič, R. Schleser, P. Studerus, T. Ihn, K. Ensslin, D. C. Driscoll, and A. C. Gossard, Phys. Rev. B **74**, 195305 (2006).
[31] S. Gustavsson, R. Leturcq, T. Ihn, K. Ensslin, M. Reinwald, and W. Wegscheider, Phys. Rev. B **75**, 075314 (2007).
[32] T. Fujisawa, T. Hayashi, R. Tomita, and Y. Hirayama, Science **312**, 1634 (2006).
[33] P. Barthold, F. Hohls, N. Maire, K. Pierz, and R. J. Haug, Phys. Rev. Lett. **96**, 246804 (2006).
[34] L. Mandel, Opt. Lett. **4**, 205 (1979).
[35] W. Belzig, Phys. Rev. B **71**, 161301(R) (2005).
[36] R. Sánchez, S. Kohler, P. Hänggi, and G. Platero, Phys. Rev. B **77**, 035409 (2008).
[37] R. Sánchez, G. Platero, and T. Brandes, Phys. Rev. Lett. **98**, 146805 (2007).
[38] T. Fujisawa, T. H. Oosterkamp, W. G. van der Wiel, B. W. Broer, R. Aguado, S. Tarucha, and L. P. Kouwenhoven, Science **282**, 932 (1998).
[39] R. Sánchez, E. Cota, R. Aguado, and G. Platero, Phys. Rev. B **74**, 035326 (2006).
[40] I. Djuric and C. P. Search, Phys. Rev. B **74**, 115327 (2006).
[41] B. Dong, H. L. Cui, and X. L. Lei, Phys. Rev. Lett. **94**, 066601 (2005).
[42] M. B. Plenio and P. L. Knight, Rev. Mod. Phys. **70**, 101 (1998).
[43] S. A. Gurvitz and Ya. S. Prager, Phys. Rev. B **53**, 15932 (1996).
[44] K. Blum, *Density Matrix Theory and Applications* (Plenum, New York, 1996).
[45] H. Carmichael, *An Open Systems Approach to Quantum Optics* (Springer-Verlag, Berlin, 1993).
[46] V. K. Zajárov, B. A. Sevastiánov, and V. P. Christiakov, *Teoría De Las Probabilidades* (Mir, Moscú, 1985).
[47] K. MacLean, S. Amasha, I. P. Radu, D. M. Zumbühl, M. A. Kastner, M. P. Hanson, and A. C. Gossard, Phys. Rev. Lett. **98**, 036802 (2007).
[48] S. Hershfield, J. H. Davies, P. Hyldgaard, C. J. Stanton, and J. W. Wilkins, Phys. Rev. B **47**, 1967 (1993).
[49] M. Gattobigio, G. Iannaccone, and M. Macucci, Phys. Rev. B **65**, 115337 (2002).
[50] A. Cottet, W. Belzig, and C. Bruder, Phys. Rev. Lett. **92**, 206801 (2004).
[51] Y. Zhang, L. DiCarlo, D. T. McClure, M. Yamamoto, S. Tarucha, C. M. Marcus, M. P. Hanson, and A. C. Gossard, Phys. Rev. Lett. **99**, 036603 (2007).
[52] S. A. Gurvitz, IEEE Trans. Nanotechnol. **4**, 45 (2005).
[53] T. Bryllert, M. Borgstrom, T. Sass, B. Gustafson, L. Landin, l.-E. Wernersson, W. Seifert, and L. Samuelson, Appl. Phys. Lett. **80**, 2681 (2002).
[54] G. Kießlich, P. Samuelsson, A. Wacker, and E. Schöll, Phys. Rev. B **73**, 033312 (2006).
[55] R. Sánchez, G. Platero, and T. Brandes, Physica E (Amsterdam) **40**, 1157 (2008).
[56] B. Elattari and S. A. Gurvitz, Phys. Lett. A **292**, 289 (2002).
[57] G. Kießlich, E. Schöll, T. Brandes, F. Hohls, and R. J. Haug, Phys. Rev. Lett. **99**, 206602 (2007).
[58] N. Lambert, Ph.D. thesis, University of Manchester, 2005.
[59] I. Djuric, B. Dong, and H. L. Cui, Appl. Phys. Lett. **87**, 032105 (2005).
[60] S. S. Safonov, A. K. Savchenko, D. A. Bagrets, O. N. Jouravlev, Y. V. Nazarov, E. H. Linfield, and D. A. Ritchie, Phys. Rev. Lett. **91**, 136801 (2003).